Journal of Mining Science, Vol. 32, No. 4, 1996

ROCK MECHANICS

PENDULUM-TYPE WAVES. PART II: EXPERIMENTAL METHODS AND MAIN RESULTS OF PHYSICAL MODELING

M. V. Kurlenya, V. N. Oparin, and V. I. Vostrikov

UDC 550.834+622.831

1. In the first part of the present work [1] a hypothesis was expressed on the basis of the main achievements in the area of nonlinear geomechanics about the possibility of the existence of a new type of elastic waves, the "elementary" carriers of which are geoblocks of various hierarchical levels due to oscillating translational and rotational movements of these blocks.

For an experimental check of this hypothesis we conducted investigations to study the characteristics of formation of elastic wave packets during pulsed excitation of models of block media by energy-calibrated impacts. In the first stage of investigations the experiments were conducted on models made of a sand—cement mixture in a 1:1 ratio. Models of two types were used. The model of the first type was a block composed of four subblocks with dimensions 297 × 295 × 290 mm and mass of 43.9 kg each. The longitudinal wave propagation velocity V_p in the concrete was on average 2460 m/sec. A plastic coupling in the form of a cord was used to provide acoustic contact between the subblocks with their horizontal arrangement. The model of the second type was a solid concrete block with dimensions 1190 × 297 × 282 mm and mass of 172 kg. Transducers of type KD 91 were attached by wax perpendicularly to the longest axis of the blocks along the centers of the side surfaces on one side of each of the subblocks in the case of the composite block (or mentally singled-out surfaces of four identical "subblocks" in the case of the solid block). Type KD 49 triggering transducers were also attached by wax at a distance of 30 mm from the place of applying the energy-calibrated impacts (end surfaces of the blocks).

As the source of pulsed actions of a given energy we used a 38-mm-diameter steel ball with a mass of 226.9 g with a vertical position of the composite block on the floor (concrete floor with a linoleum interlayer); steel balls with a diameter of 15.8 and 38 mm and masses of 14 and 226.9 g — respectively with a horizontal position of the solid and composite blocks on the floor. In the latter case the composite block was located directly on the solid block.

In the first series of experiments, with a horizontal position of the models of the solid and block media, the impact energy was changed by deflecting the filament-suspended 14- and 226.9-g balls from the equilibrium position by angles of 10, 20, ..., 90°. The energy in this case was calculated by the known formula for potential energy equal, according to the experimental conditions, to the kinetic energy at the moment of collision. In the second series of experiments, with a vertical position of the models, the energy of the pulsed action was changed by changing the drop height of the 226.9-g ball from 50 to 400 mm.

The information was recorded and processed by the measuring-calculating microseismic complex described in [1]. Multichannel removal of the information from the various models was accomplished by means of transducers with recording in an analog form on a four-channel tape recorder; conversion of the analog record to digital with obtainment of the spectral characteristics of the signals was carried out. After this the informative parameters were put out in the form of graphs. Piezoelectric acceleration transducers were used as the primary detectors. In the given experiments we used KD 91 transducers with a resonance frequency of 56 kHz and gain of 0.54-0.56 mV/msec^{-2}. The signals from the transducers were amplified by Brüel and Kjaer type 2638 voltage amplifiers. The range of amplification of the amplifiers was set within 0-60 dB.

A quantitative evaluation of the change in the spectral energy distribution of the wave packets for the corresponding blocks as a function of the energy of the pulsed actions was carried out on the basis of a discrete analog of parameter τ introduced earlier in [2] for analyzing the spatial periodicities of well logs

---

Mining Institute, Siberian Branch, Russian Academy of Sciences, Novosibirsk. Translated from Fiziko-Tekhnicheskie Problemy Razrabotki Poleznykh Iskopaemykh, No. 4, pp. 3-39, July-August, 1996. Original article submitted March 15, 1996.

1062-7391/96/3204-0245$15.00

$$\tau = \int A(f)df / \int fA(f)df, \tag{1}$$

where f and A(f) are respectively the frequency and amplitude of harmonics of the spectral image of the analog signal. Parameter τ in the given case, evidently, can be regarded as a quantity proportional to the weighted average period of the wave packet.

As a measure of the energy action on the block system we used the dimensionless parameter

$$k = \frac{W}{MV_p^2}, \tag{2}$$

where W is the energy of the pulsed action; M is the mass of a single block (subblock); V_p is the longitudinal wave velocity in the solid block. In connection with expression (2) the question arises: what do we mean by parameter W — the energy being applied by the ball at the moment of collision or the energy being absorbed by the block from the pulsed action? Although a proportionality exists between these two types of energy, an exact determination of the energy being absorbed by the excited blocks is impossible due to "imperfection" of the contact conditions between the colliding bodies. Nevertheless, an estimate for the energy from the pulsed action being absorbed by the blocks, determined with consideration of the rebound of the falling balls from the blocks on which the impact is applied, can, evidently, serve as a sufficiently good approximation.

Owing to the very large volume of graphs (several hundred) obtained as a result of the experiments, we will not dwell here on a detailed analysis of the appropriate samples of the experimental data. We will limit ourselves just to an illustration of certain most important, from our viewpoint, features related to regularities of the evolution of the spectra and characteristics of the change in parameter k according to formula (2) under the condition that the kinetic energy of movement of the balls at the moment of collision with the blocks is taken as W.

For a graphic representation of the difference of formation of elastic wave packets in the solid and block media, Fig. 1 gives typical oscillograms recorded in the solid block at various distances from the place of applying the impacts; Figs. 2 and 3 — respectively in the composite blocks located horizontally and vertically relative to the underlying surface. An analysis of the graphs shows that whereas the characteristic changes in the wave packets and their amplitude-frequency characteristics for the solid block (Fig. 1) are in essence "monotonic" and correspond to the known theoretical notions, we run into a fundamentally different situations in the case of the block models (Figs. 2 and 3). As we see from the recordings of the oscillograms, with distance from subblock to subblock the broadband (with respect to spectral energy distribution) initial seismic pulse is successively transformed into a wave packet with a line spectrum. The second (in the adopted sequence) block becomes of resonator mainly of harmonics f_i commensurate with the fundamental natural frequency $f_0 = V_p/2\Delta$ [3] of the subblock relative to the longitudinal wave and its linear dimension Δ in the direction of maximum sensitivity of the accelerometers:

$$f_i = \alpha^i f_0;\ i = 0, 1, 2, \ldots;\ \alpha = \sqrt{2}. \tag{3}$$

In the third block strong "suppression" of these frequencies occurs with simultaneous amplification of the low-frequency harmonics $\hat{f}_i$ with respect to f_0:

$$\hat{f}_i = f_{0\frac{1}{\alpha^i}};\ i = 1, 2, \ldots;\ \alpha = \sqrt{2}. \tag{4}$$

In essence "pumping" of energy from the high-frequency components of the pulse to the low-frequency ones occurs. It is noteworthy that in this block for the first time the amplitude of "infrasonic" frequencies $\hat{f}_i$ is comparable or greater than the "overtones" f_i of the initial seismic pulse, and in the fourth block exceeds the latter by more than an order. The formation of the wave with low carrier frequencies $\hat{f}_i$ is practically completed from this moment.

The described sequence of the evolution of the spectrum of recorded wave packets for vertical and horizontal composite blocks is typical for $k \in \theta_1 \cdot 10^{-11}$-$\theta_2 \cdot 10^{-9}$, with some correction for the fourth subblock of the horizontal model of the composite block: in the latter case the block is in a "free" state and the picture is substantially blurred by the additional superposition of high-frequency longitudinal and transverse waves comparable in amplitude reflected from the free surface.

An analysis of all primary information permits the conclusion that with an increase of the energy characteristic of the pulsed actions k the first signs of formation of a low-frequency wave (we denote it the μ-wave) are observed only for $k \geq \theta_1 \cdot 10^{-11}$ ($\theta_1 \geq 4$). The initial phase of this wave becomes clearly expressed at energies W corresponding to $k \cong \theta_2 \cdot 10^{-9}$, $\theta_2 \in$ 1-4 (Fig. 4). For $k \cong 4 \cdot 10^{-9}$ the block system enters a quasi-resonance operating mode as a whole: in this state the

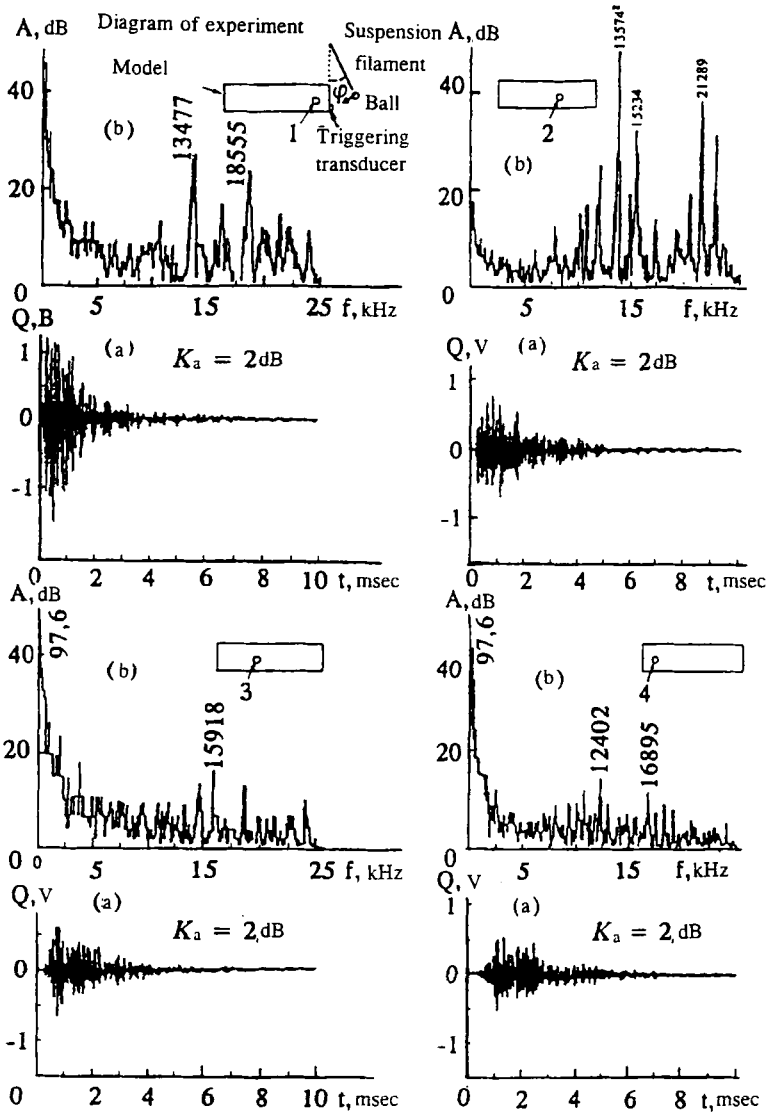

Fig. 1. Characteristic change in the form of the wave packet (a) and its amplitude-frequency spectrum (b) with distance (transducers 1-4) from the place of pulsed action of the solid block; m = 226.9 g, W = 0.673 J.

analog signals are quite substantially enriched in high-frequency components compared with adjacent energy ranges, which is indicated by the local minimum of parameter τ in Fig. 4 for all subblocks of the composite blocks. The authors regarded as the most important result of the first stage of investigations on the concrete models the detection of the effect of a canonical relationship of the spectral modes f_0 in the wave packets for each subblock of the composite blocks in modulus $\sqrt{2}$ in accordance with empirical formulas (3), (4). This circumstance does not follow at all from the known theoretical notions of the dynamic theory of elasticity [3], according to which the wave packets inside the blocks Δ (cubic approximation) for pulsed actions, first, have a frequency set f_i of type $i \cdot f_0$ (i = 1, 2, 3, ...) and, second, is bounded below by $f_0 = V_p/2\Delta$. That is, we have a far from complete set of frequency harmonics possible from a mathematical viewpoint (from the standpoint of Fourier analysis). Moreover, the spectral modes occurring in physical experiments have a specific relationship with respect to type (3)-(4).

The nontrivial facts noted above directly concerning interpretation of the mechanism of occurrence of waves of the pendulum type compelled the authors to expand the set of experimentally recorded parameters and to check relations (3), (4) for the example of block models of a different material composition and size.

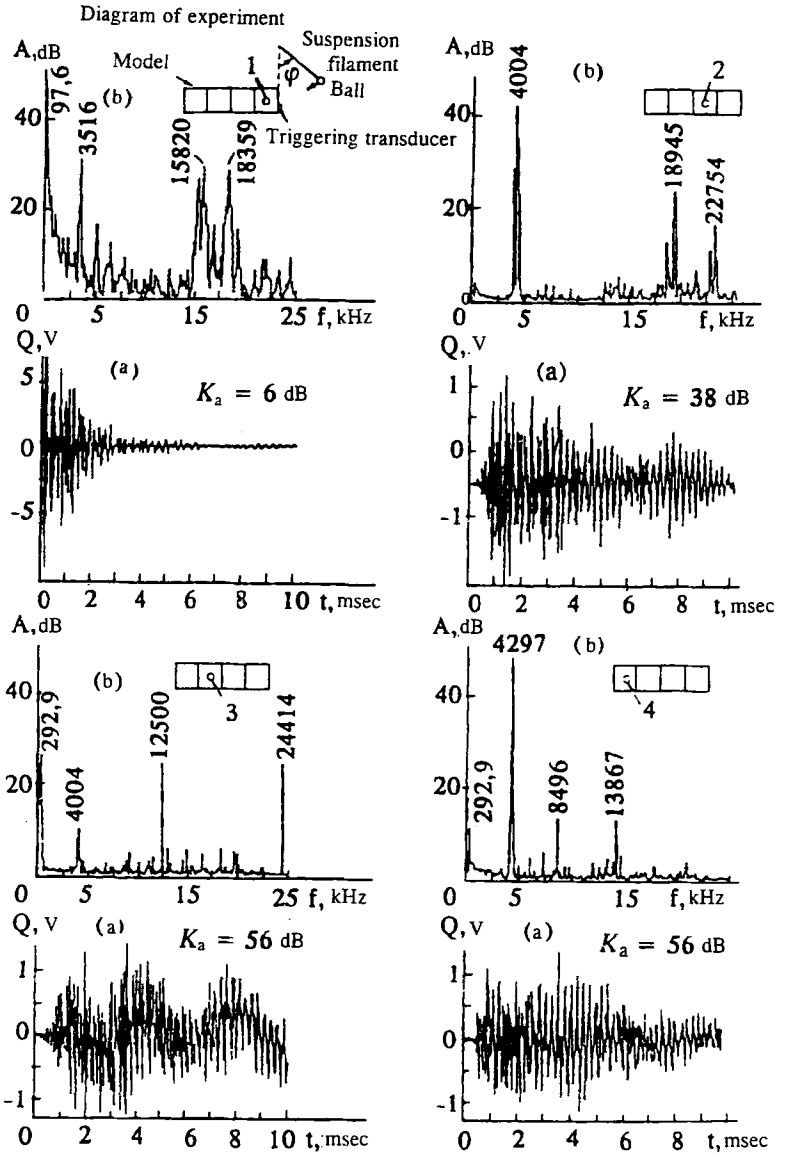

Fig. 2. Characteristic change in the form of the wave packet (a) and its amplitude-frequency spectrum (b) in a horizontal composite block: 1-4) numbers of the subblock from the place: m = 226.9 g, W = 0.315 J.

2. In this connection, in the second stage of investigations the experiments were conducted on models made of organic glass and silicate brick. Three models, shown in Fig. 5a, were used for conducting experiments at the given stage of investigations.

Model 1 is an organic glass parallelepiped with dimensions 625 × 250 × 85 mm and mass of 16.25 kg. Model 2 consists of six identical organic glass blocks with dimensions 250 × 125 × 85 mm and mass of 3.25 kg each. Model 3 is a system of six silicate brick blocks with dimensions 250 × 125 × 85 mm and mass of 5.43 . each.

When conducting the experiments the models were placed on a rubber mat lying on a concrete floor with a linoleum covering. In the given models we measured the velocity of longitudinal oscillations by the pulsed method, which was: 2814 m/sec on organic glass and 2662 m/sec in the silicate brick.

A hardened screw which served as the "point" of excitation was placed at point "*a*" on the end surface of the models. The role of the external pulsed action was played by a hardened steel striker with mass m = 82.71 g. To assign a different energy of pulsed excitation the striker was dropped from different heights from the end surfaces of the models: 16.47, 76.5,

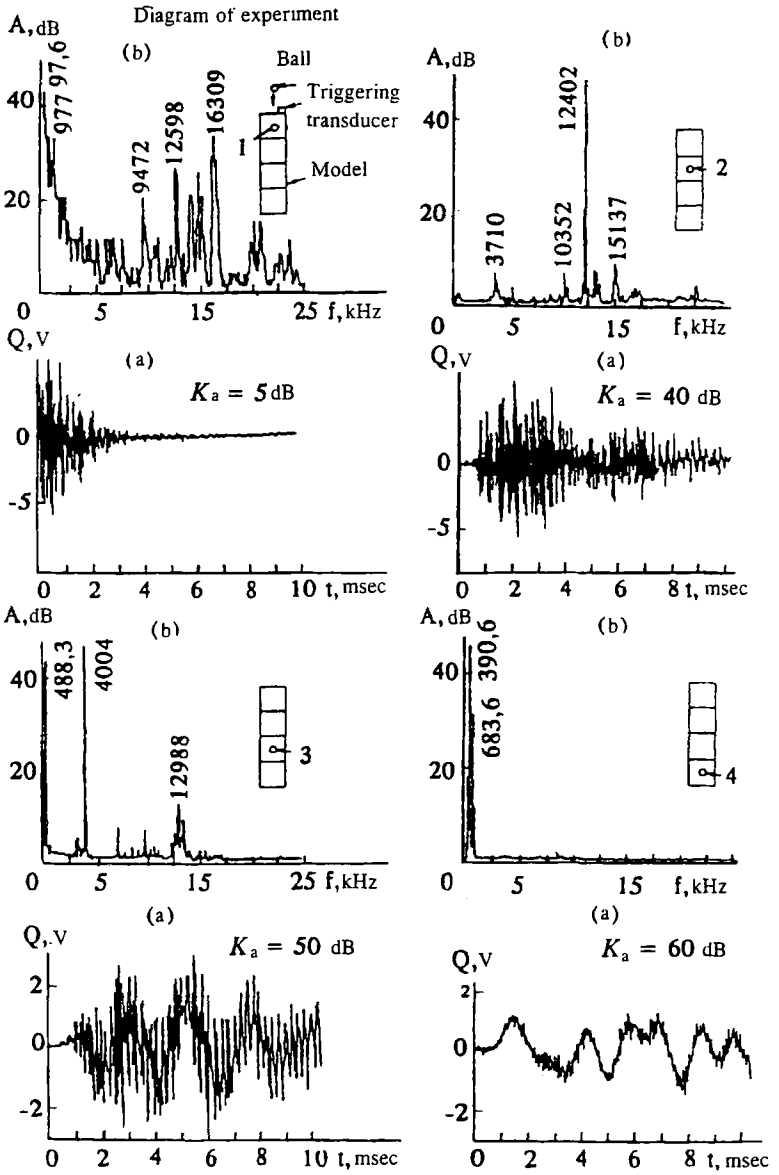

Fig. 3. Characteristic change in form of wave packet (a) and its amplitude-frequency spectrum (b) in vertical composite block: 1-4) numbers of subblocks from the place; m = 226.9 g, W = 0.222 J.

107, 136.5, 166.5, and 187 mm*. When measuring absolute displacements the striker was dropped from a height of 190 mm. On the models we measured two characteristics of acceleration on all three models and absolute displacements on model 3. Acceleration was measured by KD91 accelerometers at points 1, ..., 6 for three mutually perpendicular directions (Fig. 5b). Displacements were measured at points 1-5 by displacement transducers specially developed at the mining geophysics laboratory of the Mining Institute, Siberian Branch, Russian Academy of Sciences. A diagram of the device when conducting experiments on measuring the displacements is shown in Fig. 6.

To evaluate the degree of effect of pulsed excitation on the transducer itself, displacement was measured on the transducer after applying a blow on the model by means of an accelerometer with subsequent double integration. The value of the parasitic displacements was more than 25 dB less than the desired signal.

* The energy parameter W was calculated below with consideration of the rebound of the striker.

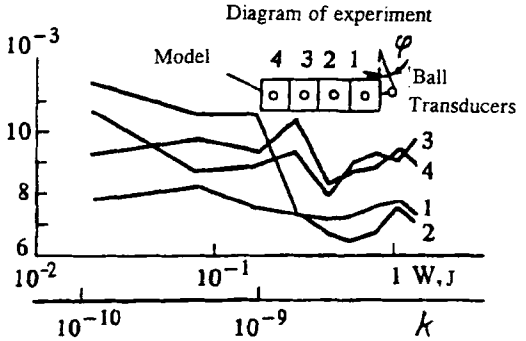

Fig. 4. Effect of energy of pulsed action on the spectral characteristic τ of wave packets.

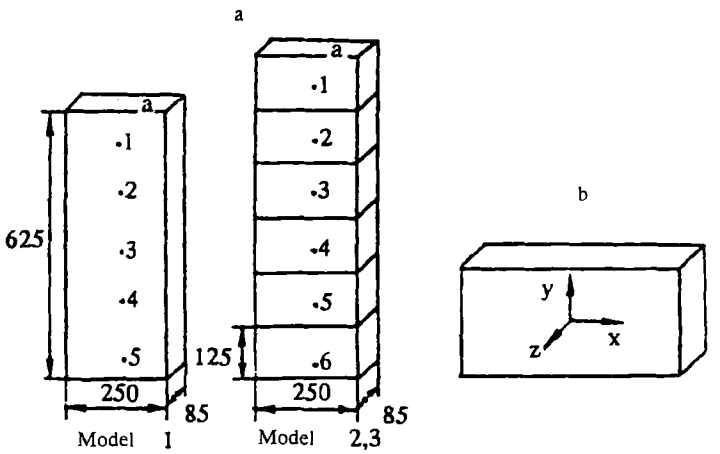

Fig. 5. Structure of models in experiments (a) and direction of recording the seismic acoustic information (b).

One of the most important tasks of the second stage of experimental investigations was to check the phenomenological relations for the spectral modes of the wave packets represented by formulas (3)-(4). Such a check was based on the following operations:

1) the values of the fundamental carrier frequencies $f_0(j)$ were calculated by the formula

$$f_0(j) = \frac{V_p}{2\Delta_j} \tag{5}$$

for each j-th direction (j ⇔ x, y, z — Fig. 5b) of the subblocks used (Δ_1 = 0.25 mm for the transverse direction (x axis); Δ_2 = 0.125 m for the longitudinal direction (y axis); Δ_3 = 0.085 m for the perpendicular direction (z axis); in the case of the solid organic glass block we used as the longitudinal dimension $\Delta_2 = 5 \times 0.125 = 0.625$ m — the length of the block);

2) the canonical frequencies $f_i(j)$ were calculated by the formula

$$f_i(j) = (\sqrt{2})^i \cdot f_0(j);\ i = 0, \pm 1, \pm 2, \ldots, \tag{6}$$

for each j-th direction of recording the acoustic data by accelerometers;

3) the canonical values $f_i(j)$ were compared with the actual modal values of the spectrograms for the appropriate records for each subblock of the models used;

4) the difference, relative to $f_i(j)$, between the canonical and actual modal values of the spectrum for the appropriate records was estimated.

Let us examine the results obtained sequentially for the three models used by us.

Model 1: solid organic glass block (Δ_1 = 0.25 m; Δ_2 = 0.625 m; Δ_3 = 0.085 m; V_p = 2814 m/sec).

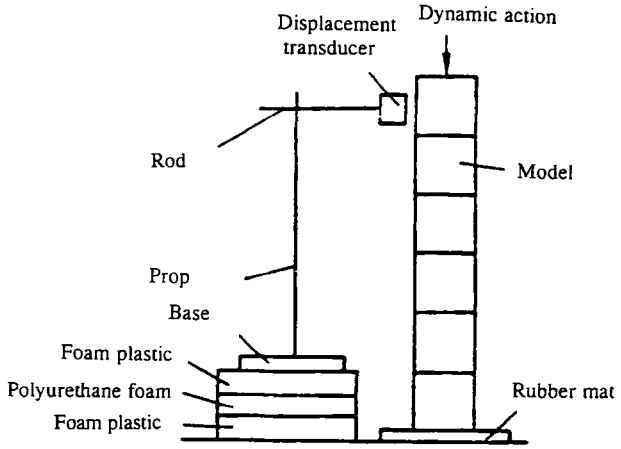

Fig. 6. Diagram of optical device when conducting experiments on measuring the absolute and relative displacements of the blocks.

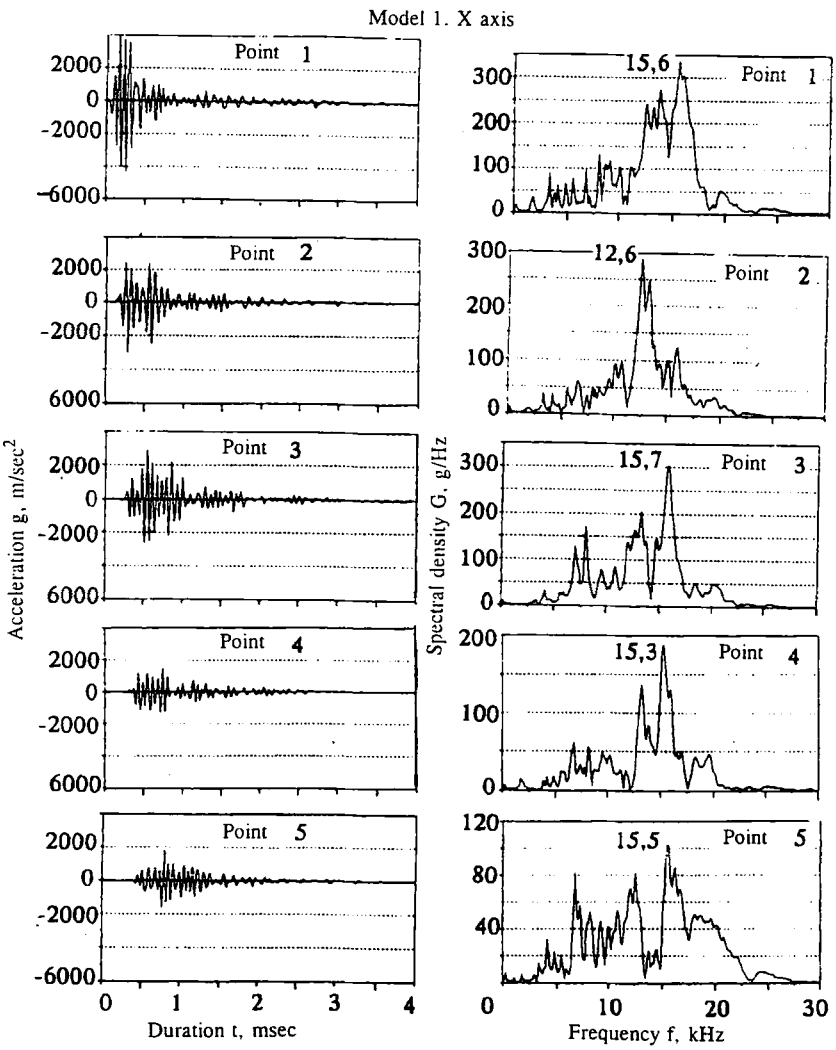

Fig. 7. Records of wave packets and their corresponding spectrograms recorded at points 1-5 of model 1 in the X direction for a pulse energy of $15 \cdot 10^{-3}$ J.

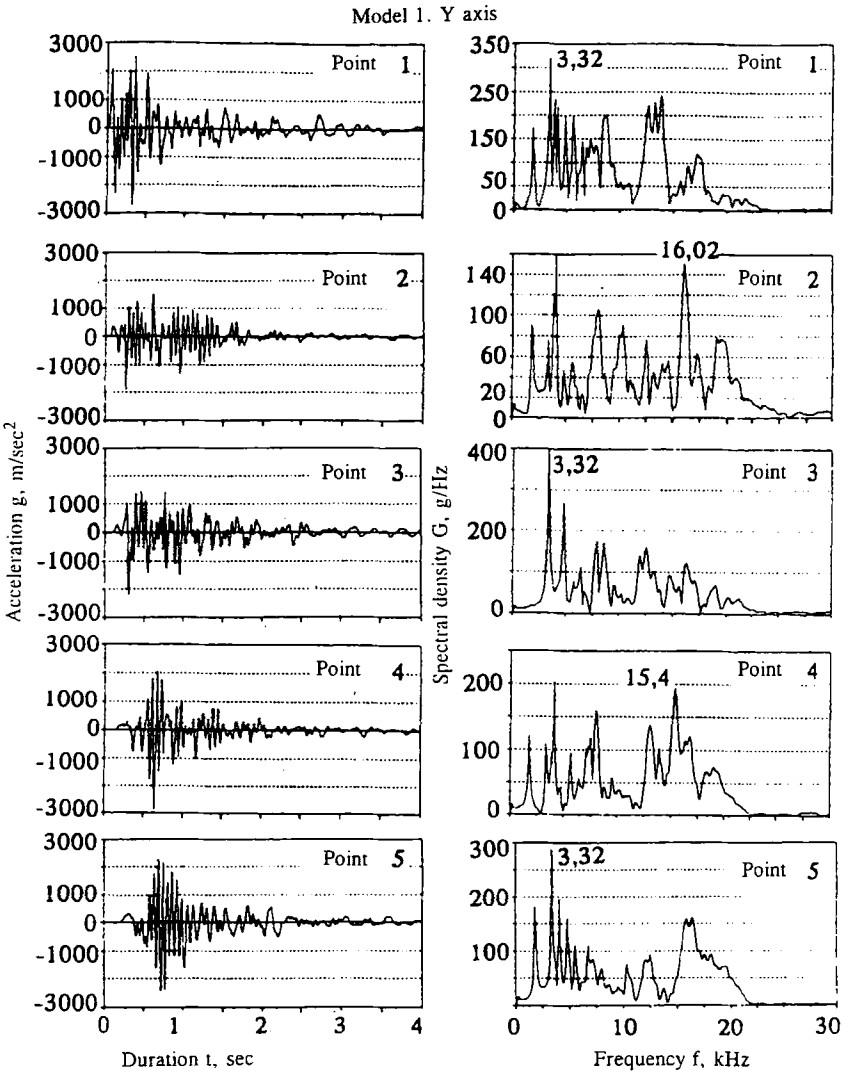

Fig. 8. Records of wave packets and their corresponding spectrograms recorded at points 1-5 of model 1 in the Y direction for pulse energy of $15 \cdot 10^{-3}$ J.

Figure 7 shows characteristic records of wave packets and spectrograms corresponding to them which were recorded in the transverse (x axis) direction by accelerometers at five equidistant points (see the diagram of the experiments above) with a pulse energy equal to $15 \cdot 10^{-3}$ J.

According to formula (5), the base frequency of oscillations for this direction ($\Delta_1 = 0.25$ m) is estimated as $f_0 \cong 5.63$ kHz. As is seen from Fig. 7, the spectral packet with such a modal value is clearly traced over all five observation points and is distinguished especially well for the records at points 2, 3, 4, 5. An analysis of the spectrograms in Fig. 7 shows that the latter in essence decompose into spectral packets with modal values corresponding to canonical frequencies f_0, $\sqrt{2}f_0$, $2f_0$, $2\sqrt{2}f_0$, $4f_0$, $4\sqrt{2}f_0$; frequencies $(1/\sqrt{2})f_0$, $1/2f_0$, $(1/2\sqrt{2})f_0$ are in a "suppressed" state. Actually, canonical frequency $f_1^+ = \sqrt{2}f_0 \cong$ 7.96 kHz corresponds to the mode of the spectral packet in the neighborhood of 7.25 kHz and is most clearly expressed for the record at point 3; for the other points it is in a suppressed state. Frequency $f_2^+ = 2f_0 \cong 11.26$ kHz corresponds to the spectral packet with a mode between marks 11.25-12.6 kHz and is traced at all measurement points. Frequency $f_3^+ = 2\sqrt{2}f_0 \cong 15.29$ kHz is in good correspondence with the mode of the spectral packet for range 15-16 kHz, being clearly traced at all measurement points (see the spectral maximum 15.4 kHz for point 4). Frequency $f_4^+ = 4f_0 \cong 22.52$ kHz corresponds to the mode of the spectral packet between marks 20-22.5 kHz and is expressed rather clearly on the records of points 1-5. Frequency $f_3^+ = 4\sqrt{2}f_0 \cong 31.8$ kHz is rather close of mode 27.5 kHz of the spectral packet for marks 25-30 kHz (the relative error is approximately equal to 13.5%): it is distinguished on the records of points 2-5. As a comparative analysis shows, the average

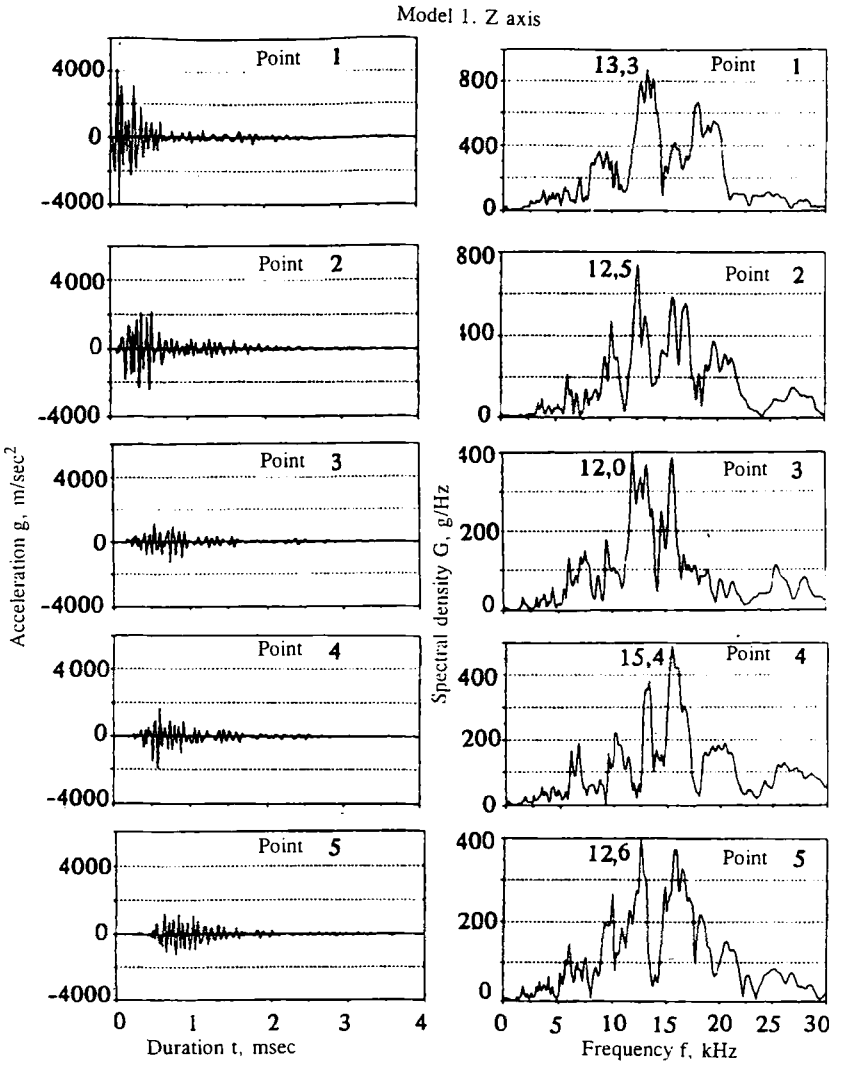

Fig. 9. Records of wave packets and their corresponding spectrograms recorded at points 1-5 of model 1 in direction Z for pulse energy of $15 \cdot 10^{-3}$ J.

relative difference between the canonical frequencies and corresponding modes of the actually detected spectral packets usually does not exceed 6%.

Figure 8 shows characteristic records of waves packets and their corresponding spectrograms for the longitudinal direction (y axis) $\Delta_2 = 0.625$ for the same characteristics of pulsed action ($15 \cdot 10^{-3}$ J) and recording system. According to formula (5), the base frequency of oscillations of the block for this direction is estimated as $f_0 \cong 2.25$ kHz. As is seen from Fig. 8, a distinct spectral maximum with close values appears on the records of points 1,2, 4, 5 — left of the mark 2.5 kHz. A general analysis of the graphs shows that the spectrograms, as in the case with Fig. 7, also decomposes into spectral groups with modal values corresponding to canonical frequencies f_0, $\sqrt{2}f_0$, $2f_0$, $2\sqrt{2}f_0$, $4f_0$, $4\sqrt{2}f_0$, $8f_0$. Actually, a distinct spectral maximum at frequency 3.32 kHz at all control points corresponds to canonical frequency $f_1^+ = \sqrt{2}f_0 \cong 3.18$ kHz. To frequency $f_2^+ = 2f_0 \cong 4.5$ kHz corresponds a pronounced spectral maximum left of mark 5 kHz at all measurement points and especially clearly at point 3: to the right of the spectral maximum at 3.32 kHz. Frequency $f_3^+ = 2\sqrt{2} \cong 6.36$ kHz is also reflected on the records of measurement points 1-5 with good resolution at points 3-5. Frequency $f_4^+ = 4f_0 \cong 9$ kHz is clearly detected on the records of points 1-3 for the spectral group of range 8-10 kHz. Frequency $f_5^+ = 4\sqrt{2}f_0 \cong 12.73$ kHz is clearly expressed on records of points 1-5 with a modal value of the spectral packet of about 12.5 kHz. Frequency $f_6^+ = 8f_0 \cong 18$ kHz corresponds well to the modal value of the spectral group in the interval 15-20 kHz. The relative difference between the canonical frequencies and modal values of the corresponding spectral groups also does not exceed 6-10%.

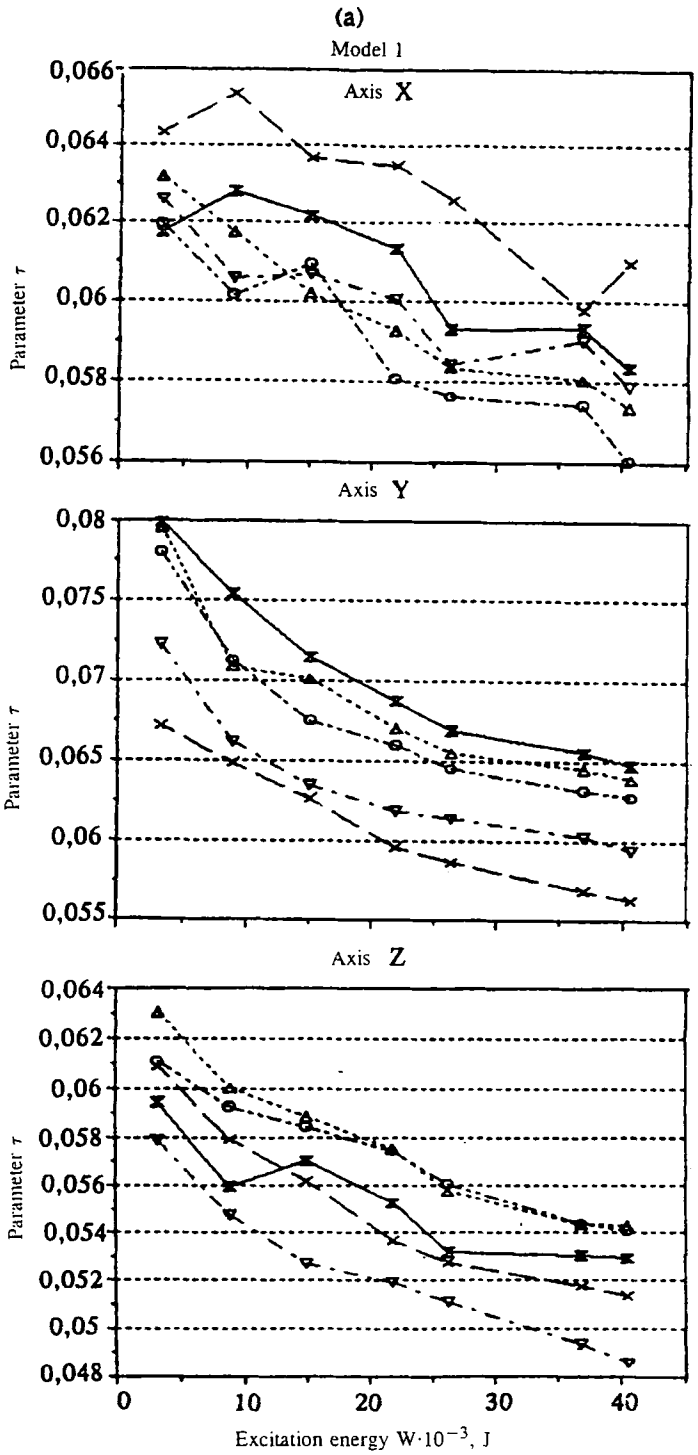

Fig. 10 (continued)

Figure 9 shows characteristic records of wave packets and their corresponding spectrograms recorded for the perpendicular direction (z axis) $\Delta_3 = 0.085$. The pulse energy from dropping the striker is $15 \cdot 10^{-3}$ J. According to formula (5), the base frequency of oscillations of the block for this direction is estimated as $f_0 \cong 16.55$ kHz. As we see from Fig. 9, a modal value of the spectral group in the range 15.3-15.7 kHz corresponds to this frequency with a relative difference of less than 6% for all measurement points: spectral maxima 15.3, 15.4, 15.5, 15.7 kHz are clearly detected on the records of these points. The spectrograms given in Fig. 9, just as in the preceding cases, in essence decompose into spectral groups

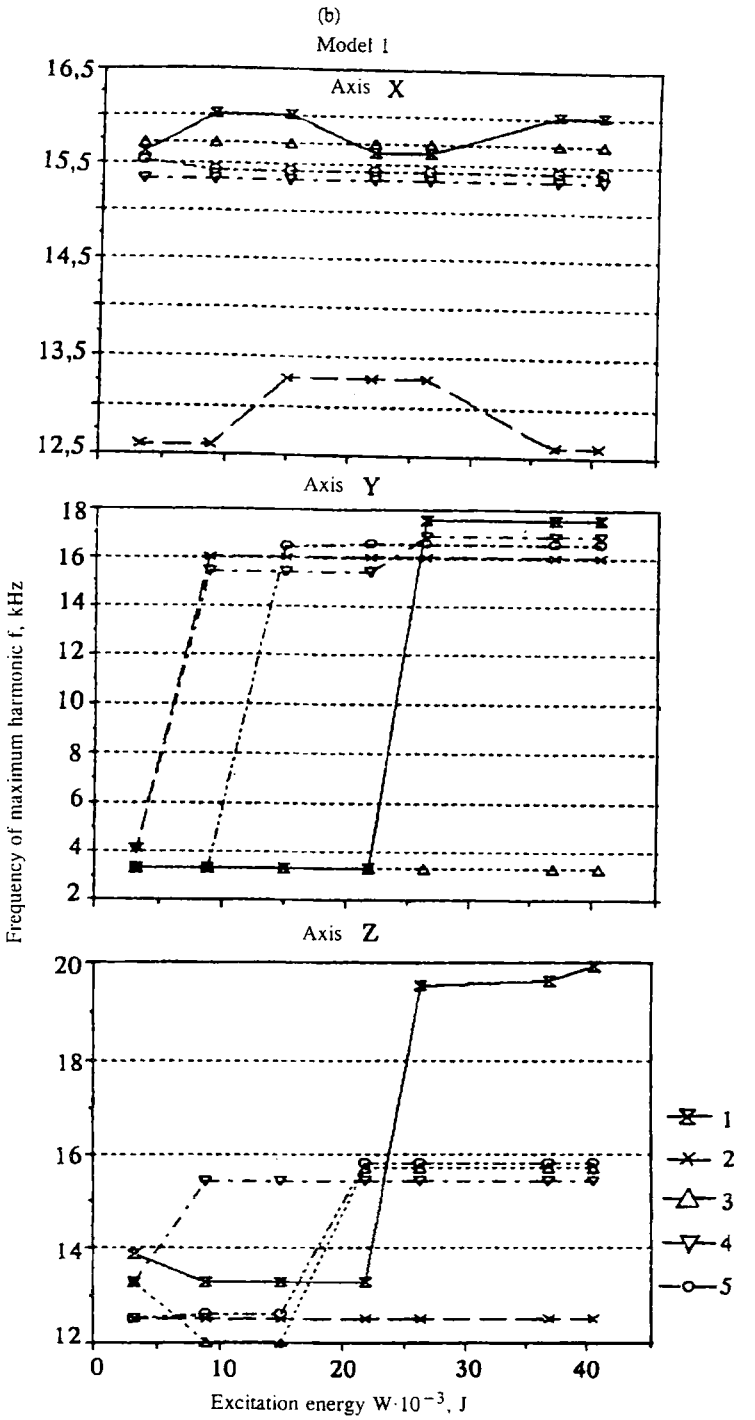

Fig. 10. Graphs of the change in parameter τ (a) and maximum frequency of the wave packets (b) as a function of the excitation energy of model 1.

corresponding to canonical frequencies f_0, $\sqrt{2}f_0$, $(1/\sqrt{2})f_0$, $1/2f_0$ and $(1/2\sqrt{2})f_0$. Actually, canonical frequency $f_1^+ = \sqrt{2}f_0 \cong$ 23.41 kHz corresponds with a relative error of not more than 10% to the modal value of the spectral group in the vicinity of 20 kHz (points 1-5). Frequency $f_1^- = (1/\sqrt{2})f_0 \cong 11.7$ kHz corresponds with an error less than 8% to the modal value of the spectral group in the vicinity of 12 kHz: a spectral maximum is clearly detected on the records of points 2-5 at mark 12.6 kHz. Frequency $f_2^- = 1/2f_0 \cong 8.28$ kHz is distinctly detected on the records of all measurement points and especially clearly for points 3-5. Frequency $f_3^- = (1/2\sqrt{2})f_0 \cong 5.85$ kHz and lower ones are in a suppressed state.

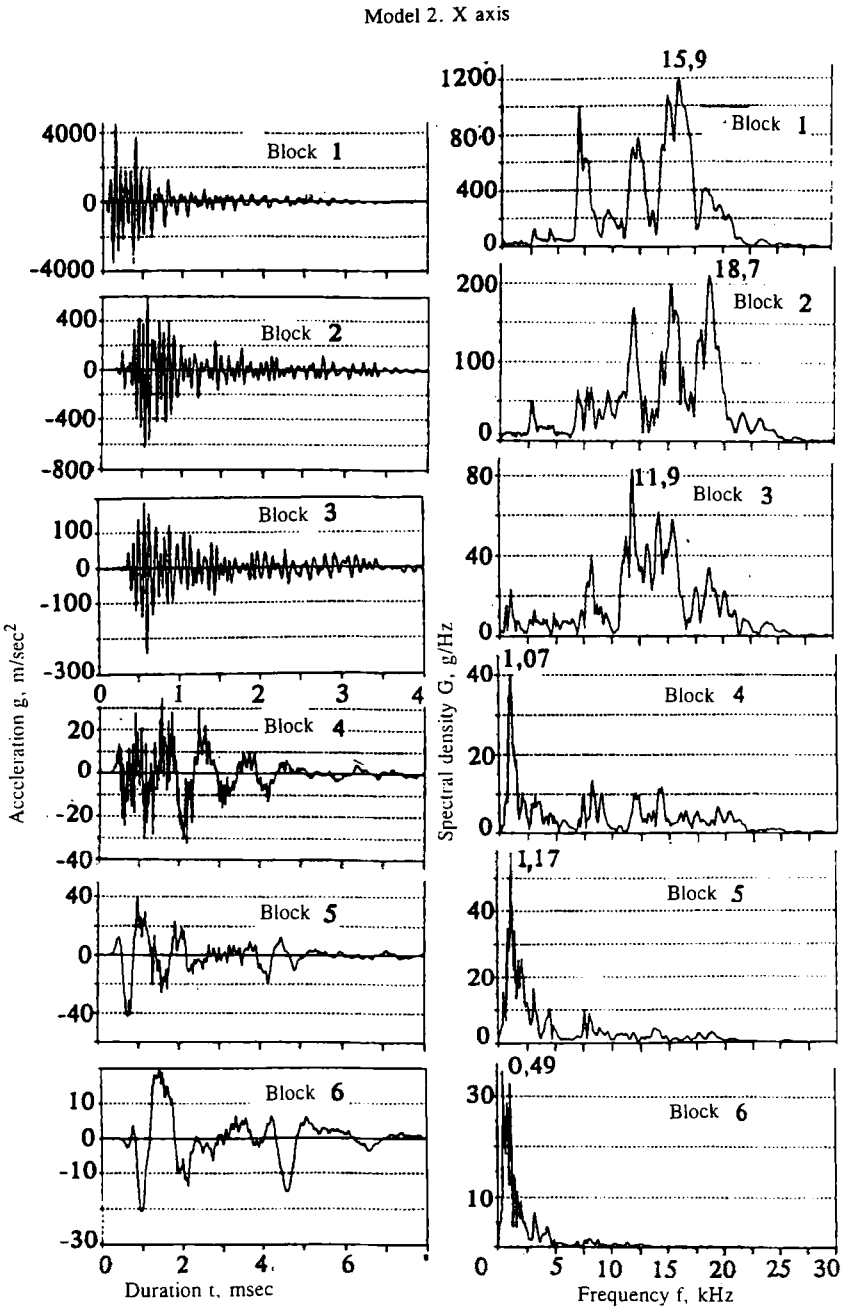

Fig. 11. Records of wave packets and their corresponding spectrograms recorded in blocks 1-6 of model 2 in the X direction for pulse energy of $15 \cdot 10^{-3}$ J.

It should be noted that the examples of records of oscillograms and spectrograms for the model of the organic glass block given above we called typical because for other cases the canonical relationship of the spectral modes is preserved with respect to the levels of energy actions (h, the drop height, changes), but in this case their amplitude values changes in favor of low-frequency harmonics. An idea about the character of such an evolution is given by Fig. 10, which shows graphs of the change in parameter τ according to formula (1) — Fig. 10a, as well as the behavior of the maximum frequency of the records of the wave packets (Fig. 10b) as a function of the excitation energy.

Consequently, the experimental data convincingly indicate the validity of formulas (3)-(4) regarding the canonical relationship of the spectral modes for wave packets forming in a solid organic glass block, the form of which substantially depends both on the linear dimension of the block and longitudinal wave propagation velocity V_p in it and on the energy of

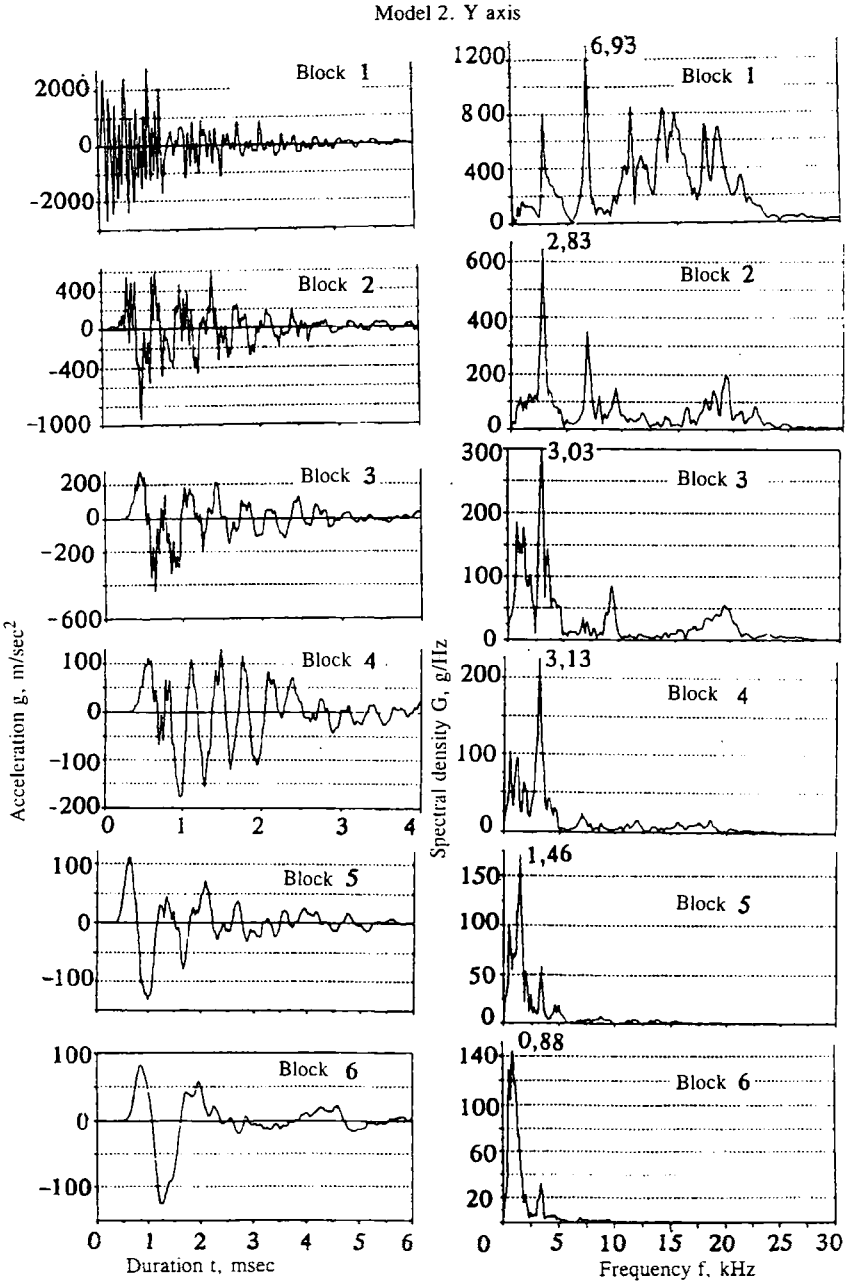

Fig. 12. Records of wave packets and their corresponding spectrograms recorded in blocks 1-6 of model 2 in the Y direction for pulse energy of $15 \cdot 10^{-3}$ J.

the external pulsed action. Figure 10b is of independent interest and we will discuss in greater detail the information contained in it in the concluding part of this article.

Let us now proceed to a check of the validity of formulas (3)-(4) for examples of the block models.

Model 2: composite block — six organic glass subblocks with $\Delta_1 = 0.25$ m; $\Delta_2 = 0.125$ m; $\Delta_3 = 0.085$ m; $V_p = 2814$ m/sec.

Figure 11 shows characteristic records of wave packets and their corresponding spectrograms recorded for each subblock in the transverse direction (x axis) with $\Delta_1 = 0.25$ m and excitation energy equal to $15 \cdot 10^{-3}$ J. According to formula (5), the base frequency of oscillations for this direction $f_0 \cong 5.63$ kHz. The mode for the spectral group most clearly corresponding to it is distinguished on records of block 4 (a weaker resolution on the others). An analysis of the graphs in Fig. 11 also reveals decomposition of the spectrograms into spectral groups with modal values corresponding to canonical frequencies f_0, $\sqrt{2}f_0$, $2f_0$, $2\sqrt{2}f_0$, $4f_0$, $1/2f_0$, $1/2f_0$, $(1/2\sqrt{2})f_0$, $1/4f_0$, $(1/4\sqrt{2})f_0$, $1/8f_0$ and $(1/8\sqrt{2})f_0$. Actually, a distinct

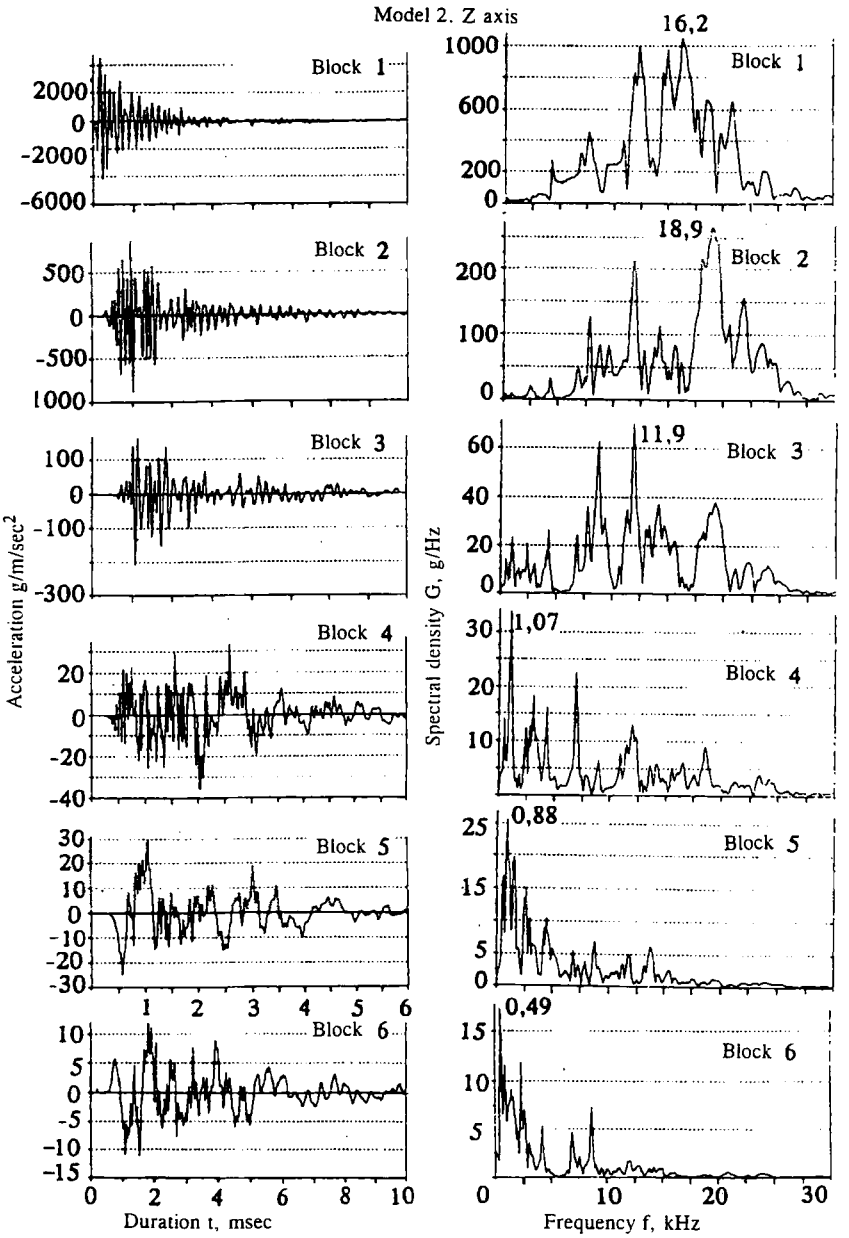

Fig. 13. Records of wave packets and spectrograms corresponding to them recorded in blocks 1-6 of model 2 in the Z direction for pulse energy of $15 \cdot 10^{-3}$ J.

spectral maximum on all blocks (especially on blocks 1-4) corresponds to canonical frequency $f_1^+ = \sqrt{2}f_0 \cong 7.99$ kHz. A sharp spectral maximum at frequency 11.9 kHz (block 3) corresponds to frequency $f_2^+ = 2f_0 \cong 11.3$ kHz. This mode is well expressed also on the records of blocks 1, 2; on block 4 — in a suppressed state; it practically disappears on blocks 5, 6. A double-peaked maximum in the range 15-16.2 kHz on block 1 corresponds to frequency $f_3^+ = 2\sqrt{2}f_0 \cong 15.92$ kHz; it is present on the records of blocks 2, 3; in a suppressed state on block 4; it practically disappears on blocks 5, 6; The maximum of the spectral group in the range 20-22.5 kHz on the records of blocks 1, 2 corresponds to frequency $f_4^+ = 4f_0 \cong 22.25$ kHz; in a suppressed state on blocks 3, 4,; it practically disappears on blocks 5, 6. A well-expressed spectral maximum left of mark 5 kHz on the records of all blocks corresponds to frequency $f_1^- = (1/\sqrt{2})f_0 \cong 3.98$ kHz. The frequency $f_2^- = 1/2f_0 \cong 2.91$ kHz is clearly expressed on the records of blocks 3-6. Frequency $f_3^- = (1/2\sqrt{2})f_0 \cong 1.99$ kHz is clearly detected on the spectral maxima of blocks 5, 6. Frequency $f_4^- = 1/4f_0 \cong 1.41$ kHz is distinguished by spectral maxima on the records of blocks 5, 6. Frequency $f_3^- = (1/4\sqrt{2})f_0 \cong 1.0$ kHz appears on the spectrogram of block 3 and clearly on the spectrogram of block 4 (peak at frequency 1.07 kHz). The spectral packet with a local maximum of 0.88 kHz on block 5 corresponds to

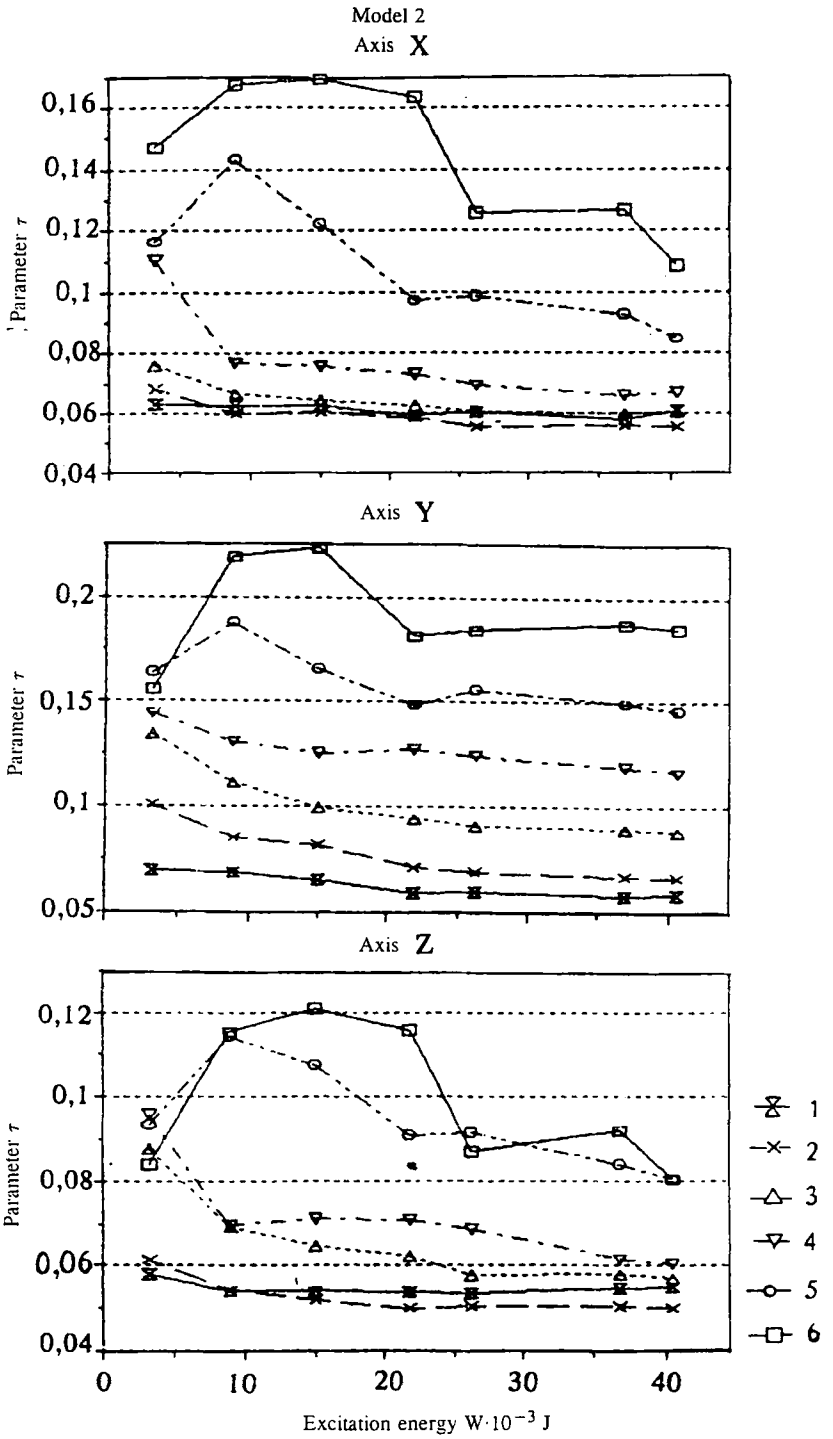

Fig. 14. Graphs of parameter τ for directions (x, y, z) for blocks 1-6 of model 2 as a function of the excitation energy.

frequency $f_6^- = 1/8f_0 \cong 0.70$ kHz; in a suppressed state on block 6. A spectral maximum at frequency 0.49 kHz for blocks 5, 6, corresponds to frequency $f_7^- = (1/8\sqrt{2})f_0 \cong 0.497$ kHz.

Figure 12 shows characteristic records of wave packets and their corresponding spectrograms recorded for each subblock of the investigated model in the longitudinal direction (y axis) with $\Delta_2 = 0.125$ m. According to formula (5), the base frequency of oscillations for this direction $f_0 \cong = 11.26$ kHz is expressed well by a spectral maximum on the record of block 1. It is easy to see that the spectrograms of the records for all blocks can be represented as spectral groups with modes

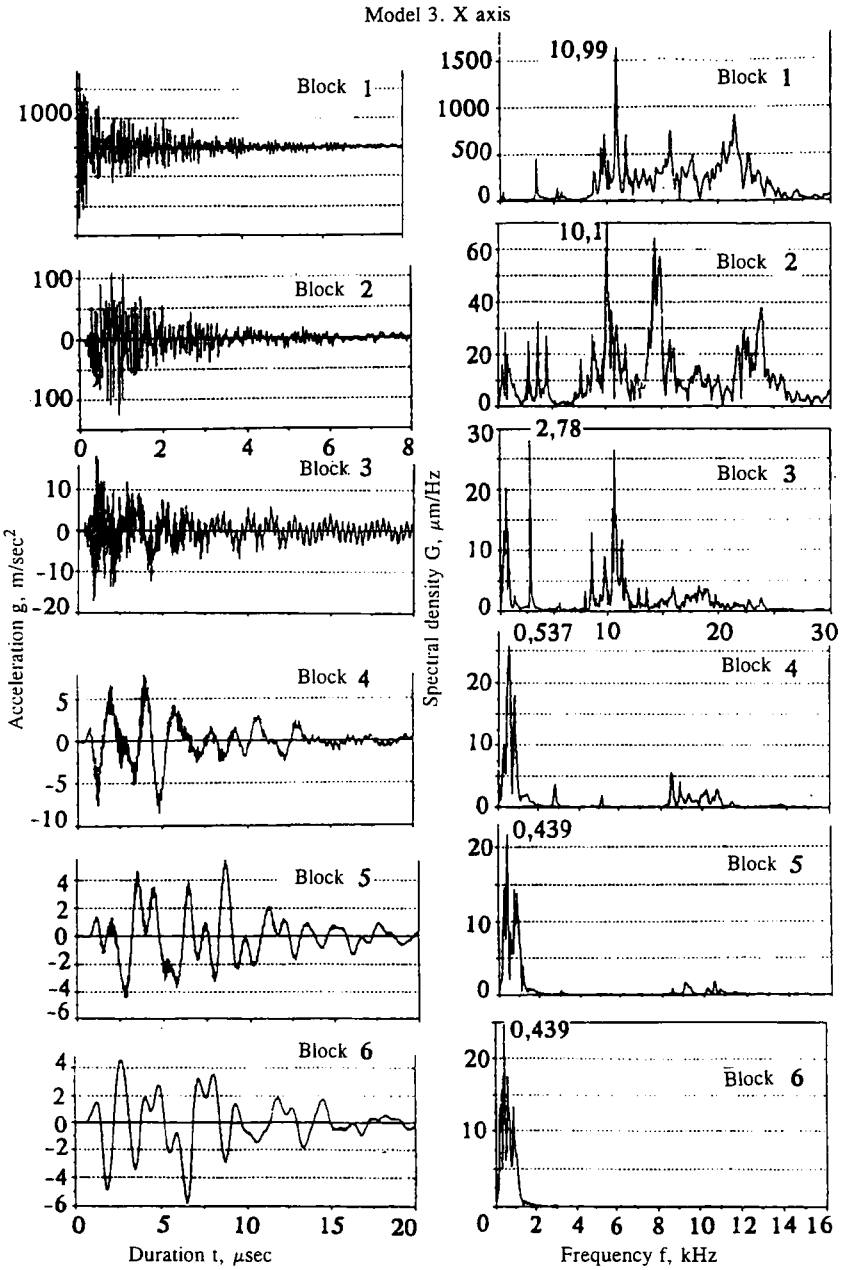

Fig. 15. Records of wave packets and their corresponding spectrograms recorded in blocks 1-6 of model 3 in the X direction for pulse energy of $15 \cdot 10^{-3}$ J.

corresponding to canonical frequencies f_0, $\sqrt{2}f_0$, $2f_0$, 1/2 f_0, 1/4 f_0, 1/8 f_0, $(1/8\sqrt{2})f_0$, 1/16 f_0. Actually, modal values of spectral groups in the range 15-17 kHz of the records of blocks 1, 2 correspond to canonical frequency $f_1^+ = \sqrt{2}f_0 \cong 15.92$ kHz; they disappear on the other blocks. The mode of the spectral group in the range 20-25 kHz corresponds to frequency $f_2^+ = 2f_0 \cong 22.5$ kHz (it is presented on the records of blocks 1, 2, it disappears on the other blocks). The spectral maximum 6.93 kHz on the records of blocks 1, 2 corresponds to frequency $f_1^- = (1/\sqrt{2})f_0 \cong 7.96$ kHz with a relative difference of 13%; it is absent on the other blocks. Spectral maximum 2.83 kHz on blocks 1, 2 correspond to frequency $f_4^- = 1/4f_0 \cong 2.82$ kHz; ≈ 3.0 kHz on block 3; ≈ 3.13 kHz on blocks 4, 5, 6 with successive suppression of this harmonic. A spectral maximum at frequency 1.45 kHz on blocks 3-5 (more expressed on block 5) corresponds to frequency $f_6^- = 1/8f_0 \cong 1.41$ kHz. Frequency $f_7^- = (1/8\sqrt{2})f_0 \cong 0.99$ kHz is reflected on spectrograms of blocks 3, 4; a spectral packet with a maximum 0.88 kHz corresponds to it on block 6. Frequency $f_8^- = 1/16f_0 \cong 0.70$ kHz appears clearly on the spectrograms of blocks 4-6.

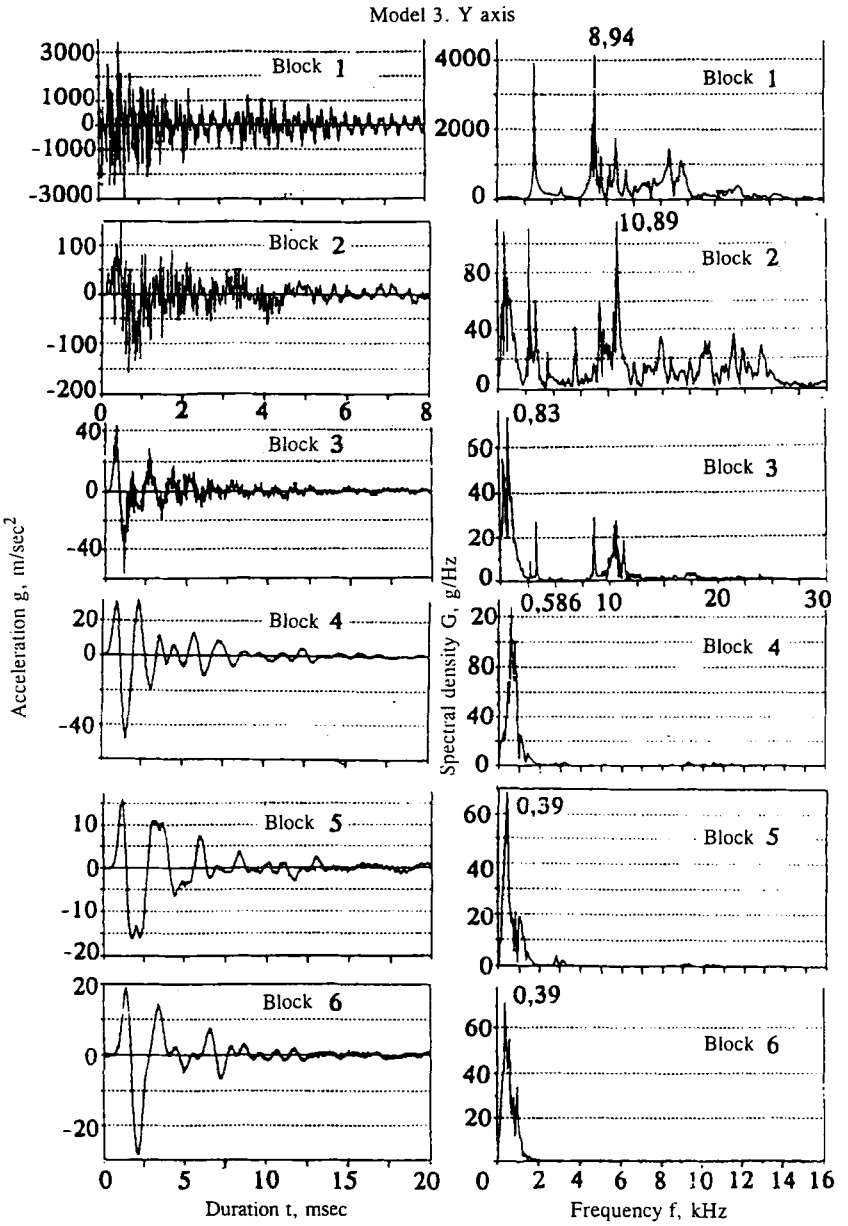

Fig. 16. Records of wave packets and their corresponding spectrograms recorded in blocks 1-6 of model 3 in the Y direction for pulse energy of $15 \cdot 10^{-3}$ J.

Figure 13 shows characteristic records of wave packets and their corresponding spectrograms recorded for the perpendicular direction (z axis) with $\Delta_3 = 0.085$ m. According to formula (5), the base frequency of oscillations for this direction $f_0 \cong 16.55$ kHz and corresponds to the spectral packet in range 15-17 kHz with a maximum 15.9 kHz on the first block. This characteristic is clearly expressed on the records of blocks 1-3; in a suppressed state on block 4; it disappears on blocks 5, 6. An analysis of the spectrograms also permits the conclusion of decomposition of the latter into spectral groups with modal values corresponding to canonical frequencies f_0, $\sqrt{2}f_0$, $(1/\sqrt{2})f_0$, $1/2\ f_0$, $1/16\ f_0$, $1/32\ f_0$. Actually, canonical frequency $f_1^+ = \sqrt{2}f_0 \cong 23.4$ kHz corresponds to the spectral maximum of the records of blocks 1-3. Here it is in a suppressed state and disappears on the records of the other blocks. Frequency $f_1^- = (1/\sqrt{2})f_0 \cong 11.7$ kHz is expressed clearly on the records of blocks 1-3, and on block 3 corresponds to spectral maximum 11.9 kHz; in block 4 in a suppressed state; it practically disappears in blocks 5, 6. Frequency $f_2^- = 1/2f_0 \cong 8.28$ kHz is detected on the records of blocks 1-3; for blocks 4, 5 in a suppressed state; it practically disappears on block 6. Frequency $f_8^- = 1/16f_0 \cong 1.04$ kHz is clearly expressed by a maximum

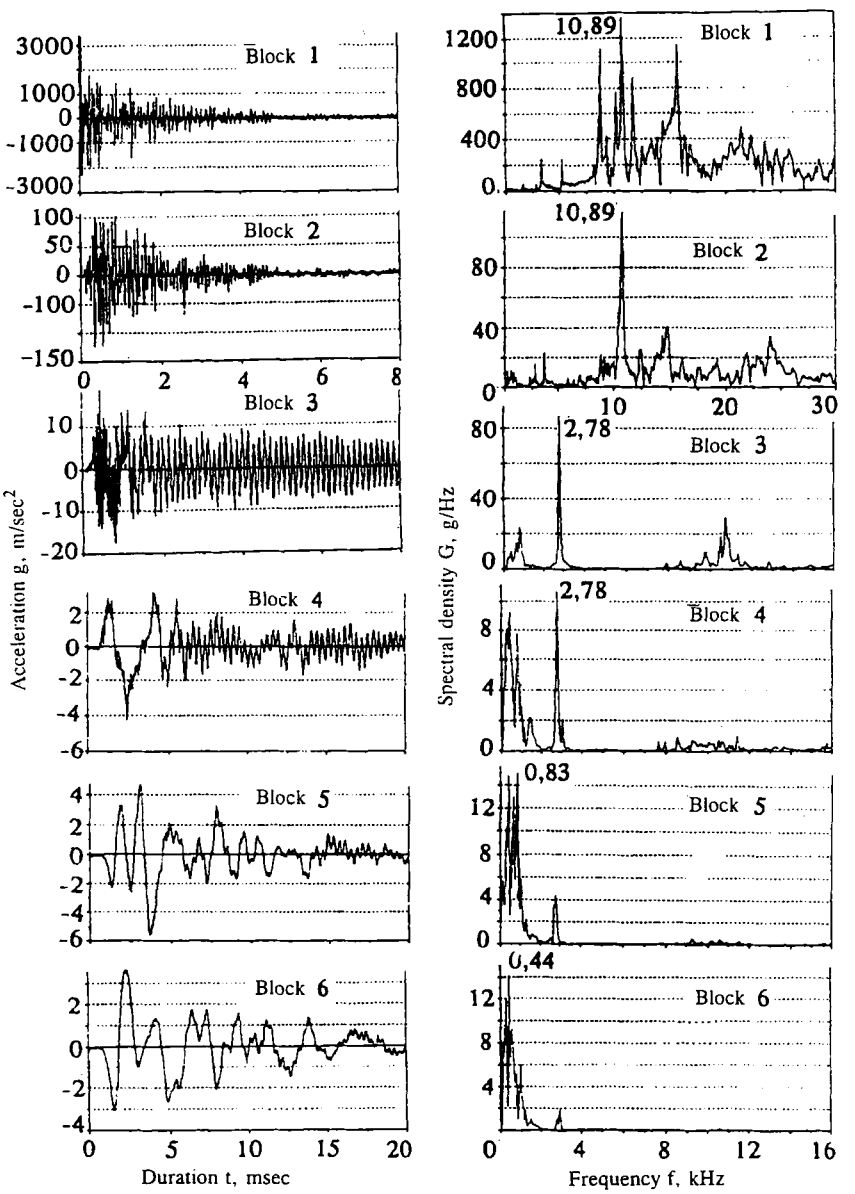

Fig. 17. Records of wave packets and their corresponding spectrograms recorded in blocks 1-6 of model 3 in the Z direction for pulse energy of $15 \cdot 10^{-3}$ J.

of the spectrograms at frequency 1.07 kHz of blocks 3, 4, and at frequency 1.17 kHz of blocks 5, 6. Frequency $f_{10}^{-} = 1/32 f_0 \cong 0.5$ kHz corresponds to a spectral maximum at frequency 0.49 kHz of block 6.

Figure 14 shows graphs of the dependence of parameter τ according to formula (1) characterizing the features of the evolution of the spectra of wave packets for the cases examined above with a different level of the energy action on the block system. Noteworthy is the propensity for working of the system of subblocks in pairs: block 6 with block 5, block 4 with block 3, block 3 with block 1, which is not surprising, considering the canonical relationship of the spectrum of waves packets in modulus $(\sqrt{2})^i$. It also follows from the given graphs with obviousness that an increase of energy of the external pulse action as a whole leads to a shift of the spectrum to the low-frequency region, although the structure of the relation of the harmonics composing the wave packets continue to remain in canonical relationship. Only their amplitude values change.

Model 3: composite block — six silicate brick subblocks with $\Delta_1 = 0.25$ m; $\Delta_2 = 0.125$ m; $\Delta_3 = 0.85$ m; $V_p = 2662$ m/sec.

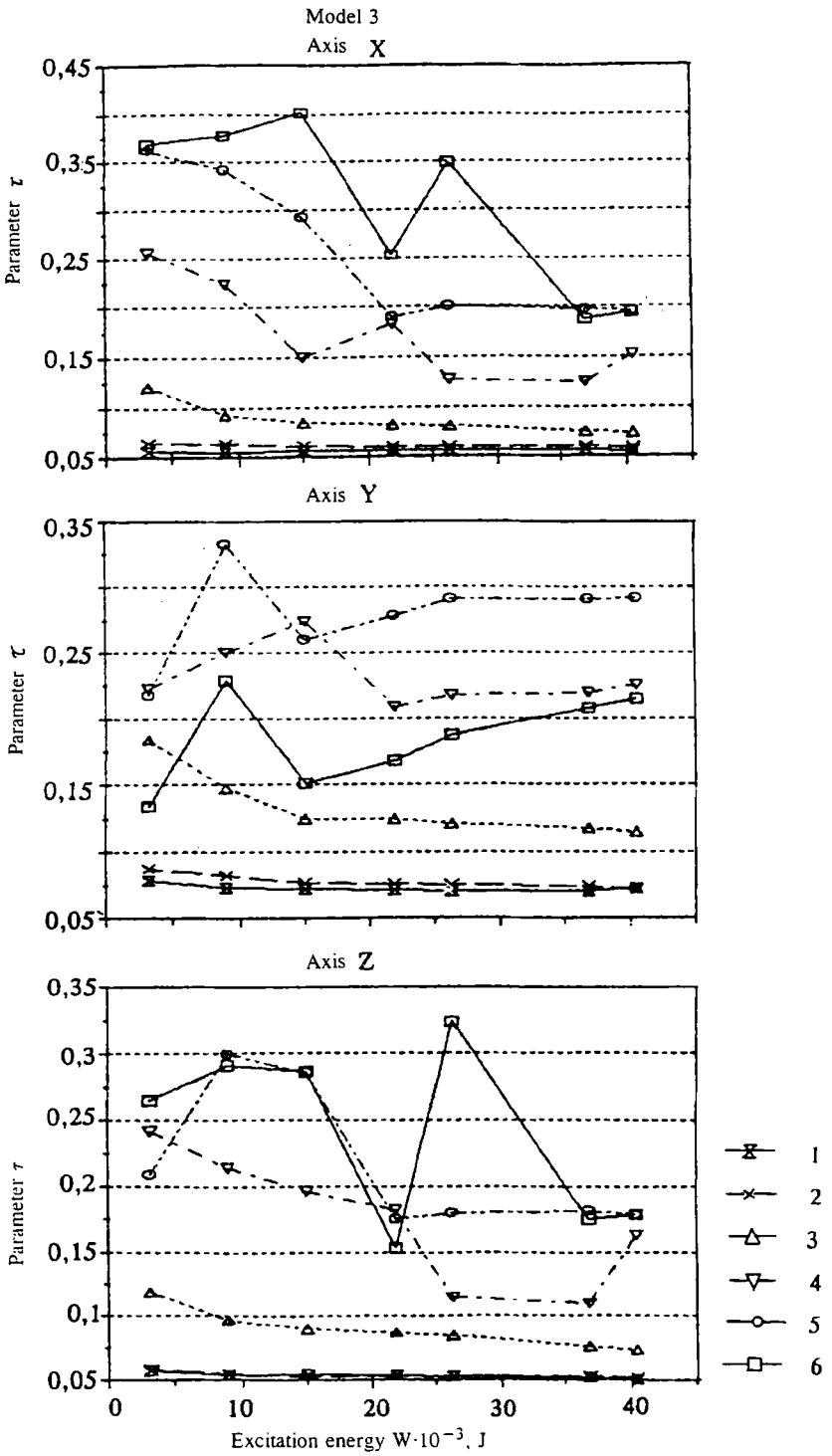

Fig. 18

Figure 15 shows characteristic records of wave packets and their corresponding spectrograms recorded for blocks 1-6 in the transverse direction (x axis) with $\Delta_1 = 0.25$ m and excitation energy $15 \cdot 10^{-3}$ J. According to formula (5), base frequency $f_0 \cong 5.32$ kHz corresponds to a distinct spectral maximum on the graph for block 1. A general analysis of the spectrograms, as in preceding cases, permits decomposing the latter into groups with modal values close to canonical frequencies f_0, $\sqrt{2}f_0$, $2f_0$, $2\sqrt{2}f_0$, $4f_0$, $4\sqrt{2}f_0$, $1/2f_0$, $1/4f_0$, $(1/4\sqrt{2})f_0$, $1/8f_0$, $(1/8\sqrt{2})f_0$, $1/16f_0$.

Thus, a sharp spectral maximum on the record for block 1 left of mark 10 kHz corresponds to canonical frequency $f_1^+ = \sqrt{2}f_0 \cong 7.53$ kHz. A sharp spectral maximum on the records of blocks 1-3 at frequency 10.89 kHz corresponds also to

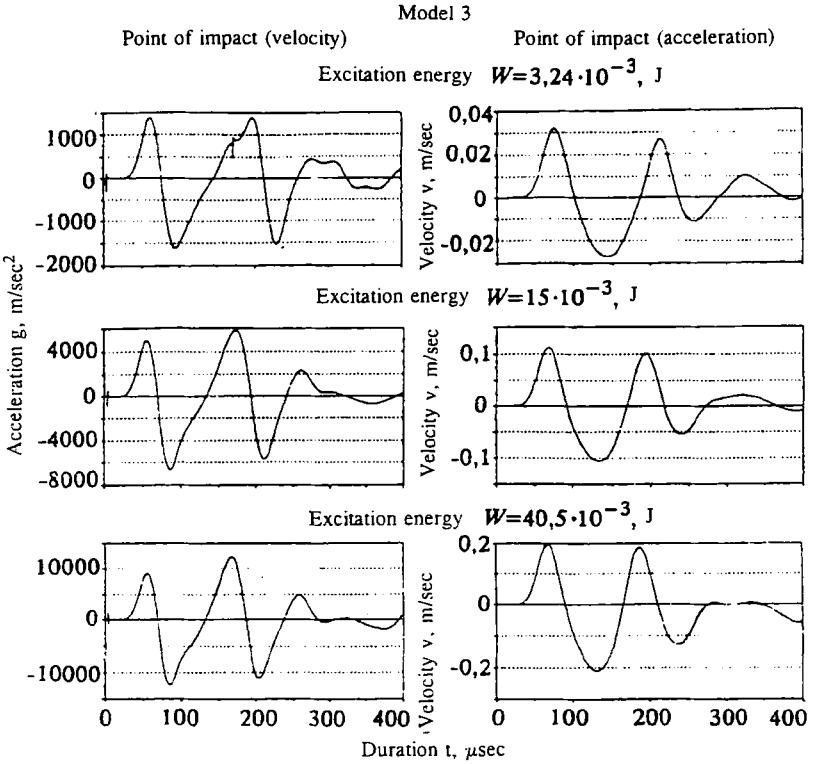

Fig. 19. Structure of the external pulsed action with respect to acceleration (a) and velocity (b) of displacement of the surface of excitation of the blocks for energies up to $40.5\cdot10^{-3}$ J.

frequency $f_2^+ = 2f_0 \cong 10.65$ kHz. It disappears on records of the other blocks. The spectral maximum on the record of block 1 corresponds to frequency $f_3^+ = 2\sqrt{2}f_0 \cong 15.06$ kHz; in a suppressed state for block 2; it disappears on the other blocks. A spectral packet in the range 20-23 kHz with a modal value close to it on the record of block 1 corresponds to frequency $f_4^+ = 4f_0 \cong 21.26$ kHz; in a suppressed state for block 2; it is absence on the other blocks. A distinct spectral maximum on the records of blocks 1, 2 corresponds to frequency $f^+{}_5 = 4\sqrt{2}f_0 \cong 30.09$ kHz; harmonics higher than 10-12 kHz are absent on the other blocks. A sharp spectral maximum at frequency 2.78 kHz of the records of blocks 3, 4 corresponds to frequency $f_2^- = 1/2f_0 \cong 2.66$ kHz; in a suppressed state on blocks 5, 6. Frequency $f_4^- = 1/4f_0 \cong 1.33$ kHz appears on block 4. A spectral group in the interval 0.8-1.0 kHz with a sharp maximum at frequency 0.83 kHz (it appears on the records of blocks 3-6) corresponds to frequency $f_5{}^- = (1/4\sqrt{2})f_0 \cong 0.94$ kHz. Frequency $f_6^- = 1/8f_0 \cong 0.67$ kHz is clearly expressed on records of blocks 5, 6. Spectral maximum 0.44 kHz clearly detected on the records of blocks 4-6 corresponds to frequency $f_7{}^- = (1/8\sqrt{2})f_0 \cong 0.47$ kHz. Frequency $f^-{}_8 = 1/16f_0 \cong 0.33$ kHz is resolved most clearly on the record of block 6. The graphs of the analog signals and their spectra for blocks 3 (especially!) and 4 call special attention to themselves. The structure of these surprising records in essence unravel the mechanism of occurrence of pendulum-type waves as the work of a unique geomechanical laser system, on one hand, and indicate the occurrence of conditions of anomalously low friction for block 3 in the perpendicular direction, on the other. By virtue of the fundamental importance of this result, we will dwell below on its more detailed discussion.

Figure 16 shows characteristic records of wave packets and their spectrograms recorded for the investigated model in the longitudinal direction (y axis) with $\Delta_2 = 0.125$ m ($15\cdot10^{-3}$ J). According to formula (5), the base frequency $f_0 \cong 10.65$ kHz. It is easy to see that the spectrogram in essence also decompose into spectral packets with modal values corresponding to canonical frequencies f_0, $\sqrt{2}f_0$, $2f_0$, $(1/\sqrt{2})f_0$, $1/2f_0$, $(1/2\sqrt{2})f_0$, $1/4f_0$, $(1/8\sqrt{2})f_0$, $1/16f_0$, $(1/16\sqrt{2})f_0$, $1/32f_0$.

Actually, distinct spectral maxima on the records of blocks 1, 2 correspond to canonical frequency $f_1^+ = \sqrt{2}f_0 \cong 15.06$ kHz (they disappear on the others). A spectral maximum clearly seen on the record of block 2 corresponds to frequency $f_2^+ = 2f_0 \cong 21.3$ kHz (it is absent on blocks 3-6). Frequency $f_1{}^- = (1/\sqrt{2})f_0 \cong 7.53$ kHz corresponds to the mode of the spectral group in interval 7.25-9 kHz on the records of blocks 1, 2 and most distinctly on the record of block 3 (the spectral maximum between marks 7.25-10 kHz). For the other blocks f_1^- disappears. A feebly expressed spectral maximum on the record of block

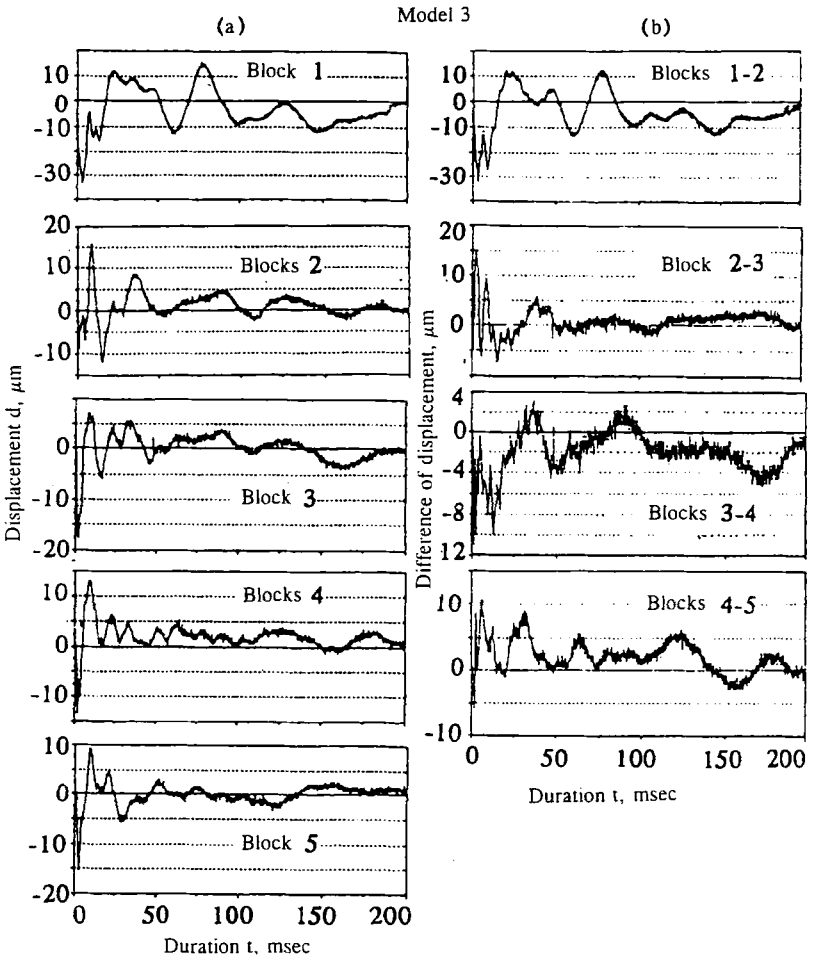

Fig. 20. Graphs of the absolute (a) and relative (b) displacements of blocks 1-5 with time for model 3 in interval 0-200 msec for excitation energy $W = 41.1 \cdot 10^{-3}$ J.

1 corresponds to frequency $f_2^- = 1/2f_0 \cong 5.33$ kHz (*it* is absent on the others). The first spectral maximum on block 1 corresponds to frequency $f_3^- = (1/2\sqrt{2})f_0 \cong 3.77$ kHz, f_3^- also corresponds to the modal values of the spectral groups in interval 3-4 kHz for the records of blocks 2, 3 (they disappear on the others). A sharp spectral maximum on the record of block 2 corresponds to frequency $f_4^- = 1/4f_0 \cong 2.66$ kHz (it is absent on the others). A pronounced spectral maximum at ≈ 1 kHz for records of blocks 4-6 (for block 3 a maximum is detected at frequency 0.83 kHz) corresponds to frequency $f_1^- = (1/8\sqrt{2})f_0 \cong 1$ kHz. Frequency $f_8^- = 1/16f_0 \cong 0.67$ kHz correlates with the mode of the spectral packet in interval 0.5-1.0 kHz for block 4 (maximum at frequency 0.586 kHz). The mode of the spectral packet in interval 0.39-0.5 kHz for block 6 corresponds to frequency $f_9^- = (1/16\sqrt{2})f_0 \cong 0.47$ kHz. A spectral maximum at frequency 0.39 kHz corresponds to frequency $f_{10}^- = 1/32f_0 \cong 0.33$ kHz on records of blocks 5, 6.

Figure 17 gives characteristic records of wave packets and their spectrograms recorded for the perpendicular direction (z axis) with $\Delta_3 = 0.085$ m. According to formula (5), the base frequency $f_0 \cong 15.7$ kHz. As is easy to be convinced, in this case also the spectrograms decompose into spectral groups with modal values close to canonical frequencies $f_1^+ = \sqrt{2}f_0 \cong 22.2$ kHz; $f_1^- = (1/\sqrt{2})f_0 \cong 11.1$ kHz; $f_4^- = 1/4\, f_0 \cong 3.9$ kHz; $f_5^- = (1/4\sqrt{2})f_0 \cong 2.78$ kHz; $f_8^- = 1/16\, f_0 \cong 0.98$ kHz; $f_{10}^- = 1/32\, f_0 \cong 0.49$ kHz and $f_{12}^- = 1/64\, f_0 \cong 0.25$ kHz. In all examples given above the relative differences between the canonical frequencies and the actual spectral maxima (or group modes) corresponding to them, as a rule, did not exceed 6%.

Figure 18 shows graphs of parameter τ for the above-examined directions of recording oscillations in blocks of model 3, giving an idea about the character of the shift of the dominant wave packets with change in the level of the energy actions on the system. Here, as in the preceding case of model 2, there is a dominant tendency toward a shift of the spectral filling of the wave packets into the low-frequency region with increase of the pulse energy. Although, as seen from Fig. 18, there

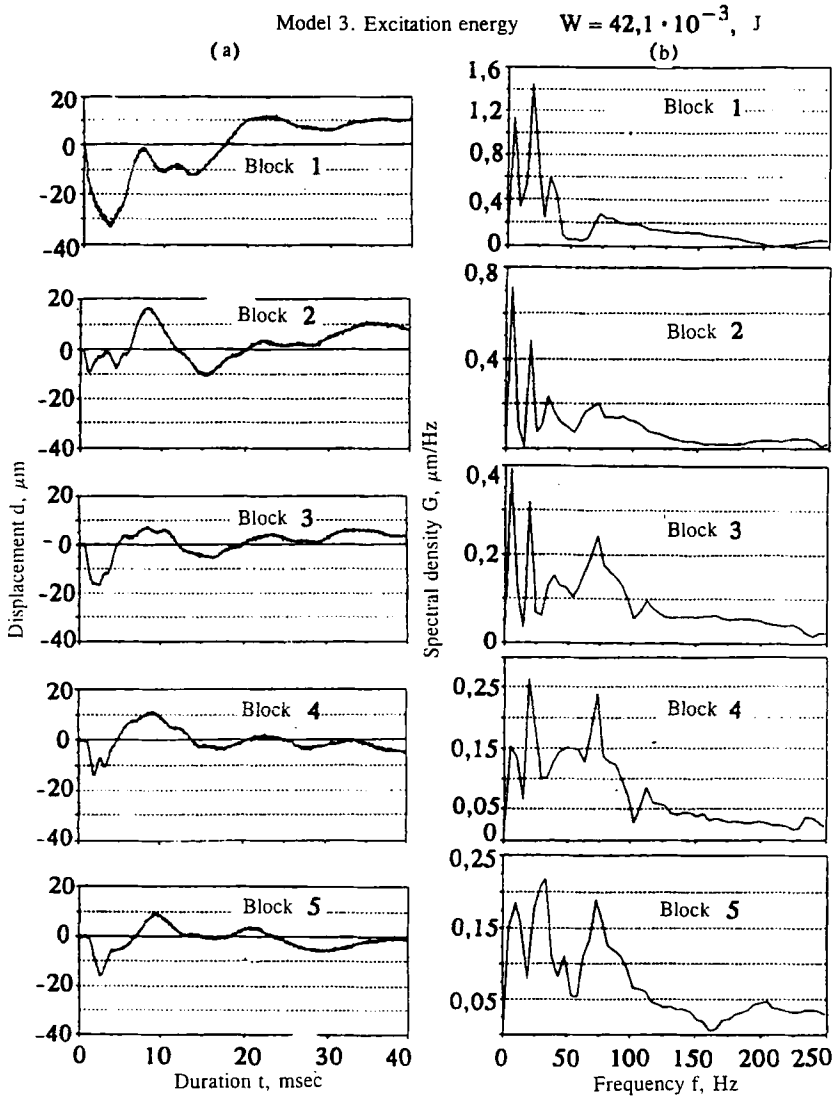

Fig. 21. Graphs of the absolute displacements of blocks 1-5 and their corresponding spectrograms of model 3 for time interval 0-40 msec for excitation energy W = $41.1 \cdot 10^{-3}$ J.

are blocks with, generally speaking, a nonmonotonic behavior for certain directions. As we will point out in the concluding section of the article, the latter circumstance contains a profound physical significance.

Thus, the analysis given above for various models of geomaterials convincingly indicate that the formation of elastic wave packets in blocks of rock masses obeys the law of canonical relationship of their spectra $\overline{f}_i$ in modulo $(\sqrt{2})^i$

$$\vec{f}_i = \vec{f}_0(\sqrt{2})^i,\ i = 0, \pm 1, \pm 2, \ldots, \tag{6}$$

where $\vec{f}_0 = \frac{V_p}{2\vec{\Delta}}$, V_p is the longitudinal wave velocity in the blocks $\overline{\Delta}$ is the characteristic dimension of the blocks. Formula (6) is given in a vector representation

$$\vec{f} = (f_x, f_y, f_z);\ \vec{\Delta} = (\Delta_x, \Delta_y, \Delta_z); \tag{7}$$

(x, y, z) are orthogonal directions for the surfaces of the blocks. Relationship (6) in essence suggests also what mathematical apparatus is most suitable for a spectral analysis of actual seismograms for the purpose of detecting real physical periodicities.

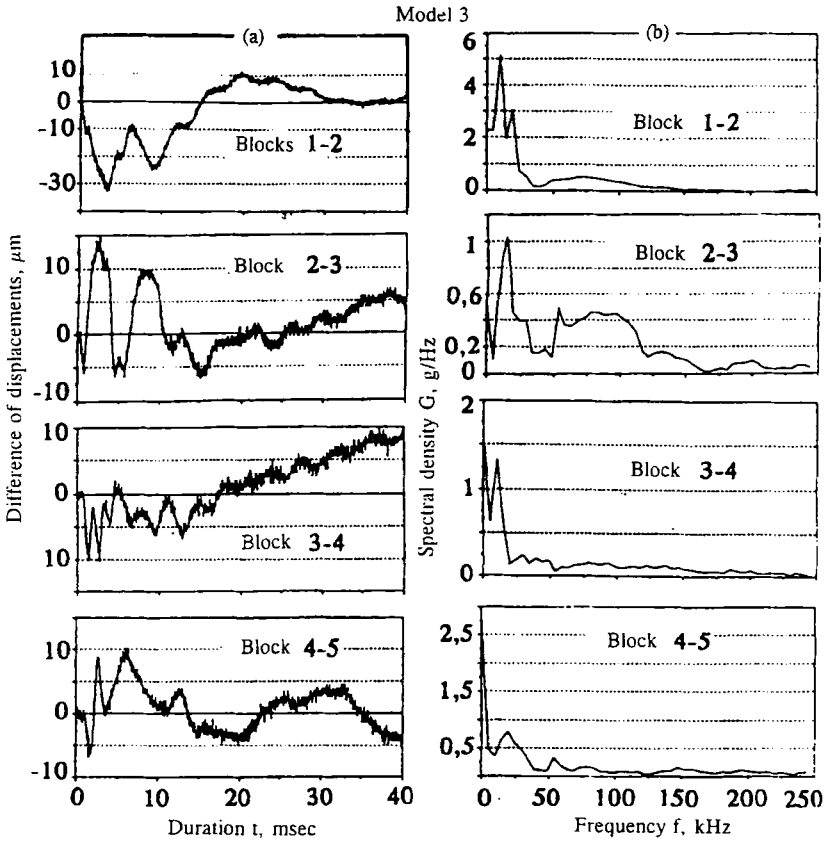

Fig. 22. Graphs of the relative displacements of blocks 1-5 and their corresponding spectrograms of model 3 for time interval 0-40 msec for excitation energy W = $4.1 \cdot 10^{-3}$ J.

Information on the spectral characteristics of the pulsed action on the surface of the first block of model 3 can be obtained from Fig. 19, which gives examples of records of acceleration and velocity* recorded by the triggering accelerometer for various energies of the pulsed action $(3.24, 15, 40.5) \cdot 10^{-3}$ J. It is easy to see that pulsed actions realized in the experiments (dropping of a steel striker with rebound) are actually equivalent to the work on the surface of the blocks of a vibrator injecting into the system a quasi-sinusoidal signal with two apparent periods $T_a \cong 107$ μsec (frequency $\hat{f}_a = 1/T_a \cong 9.4$ kHz). If we turn to Figs. 15-17 we note that $\hat{f}_a \cong 9.4$ kHz almost coincides with the modal value of the spectral groups in interval 9-10 kHz of the records in all directions and is close to the reference frequency $f_0 \cong 10.65$ kHz for the longitudinal direction (the relative difference is less than 12%). Here it is significant that an increase of the pulse energy does not lead to a considerable distortion of its form, but leads only to an increase of the corresponding amplitude characteristics (it is easy to compose this relation on the basis of the data in Fig. 18).

3. A general analysis of the evolution of the spectral filling of the wave packets in three orthogonal directions (x, y, z) for each subblock of models 2 and 3 (Figs. 11-17) permits the assumption that the general regularities detected on the records of the accelerometers (relationship with respect to the reference frequencies $\hat{f}_0$, shift of spectral packets into the low-frequency region, approximately identical structure of the records for fixed blocks in all three directions with the formation of comparable dominant low-frequency harmonics, etc.) are due mainly to the character of internal deformation of the blocks. In this connection, for convincing proof of the thesis that the geoblocks in this case move as a "whole," it was necessary to measure the graphs of the absolute displacements for each subblock. The second main task of the investigations consisted in this for model 3. It is understandable that an important task also is to obtain an answer to the question: what relationships exist between intradeformation waves of the blocks and the dynamic and kinematic characteristics of the latter in an approximation of "absolutely" solid bodies — carriers of the pendulum waves? An optical system of measurements, the structure of which is

* The velocity was calculated in accordance with acceleration.

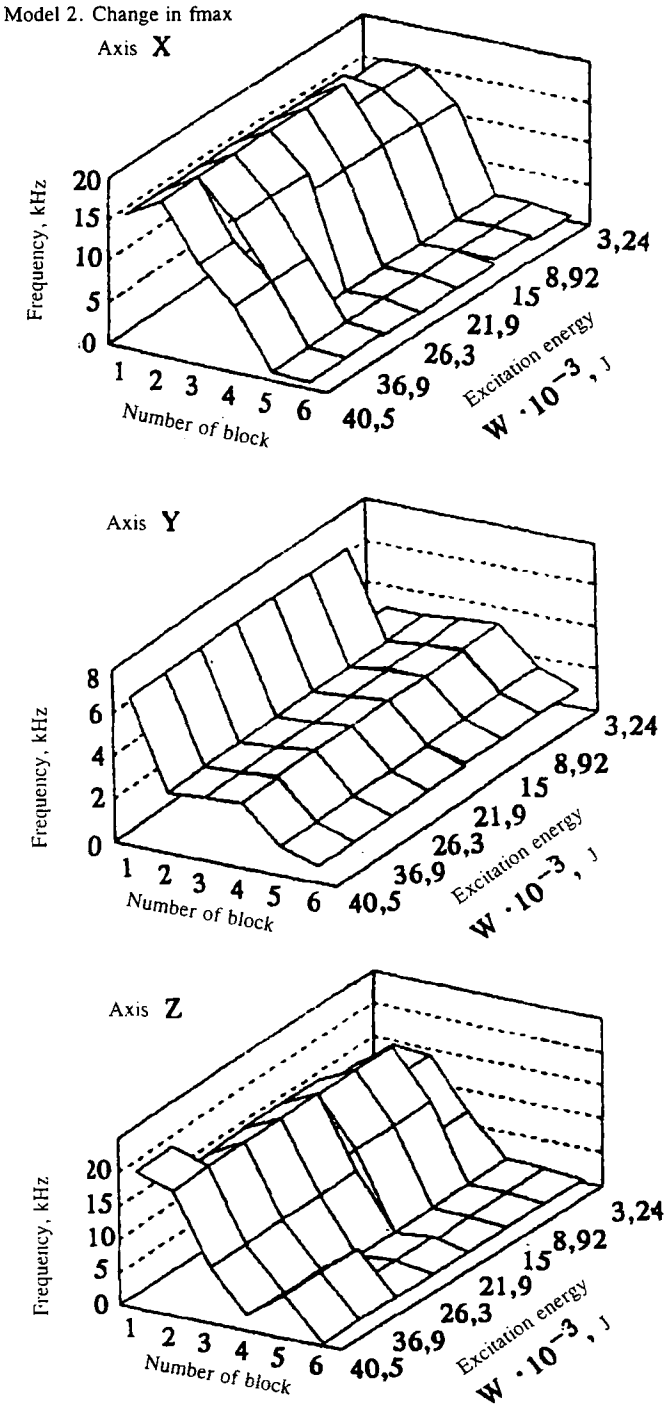

Fig. 23 (continued)

shown above in Fig. 6, was used to accomplish these tasks. The results obtained are given in Fig. 20. Given there are graphs of the changes in absolute displacements of blocks 1-5 with time for model 3 (a) and graphs of the relative displacement between adjacent blocks (b) in time interval 0-200 msec. Difference graphs (b) were obtained by subtracting graphs (a) of absolute displacements for subblocks j from the graphs of the absolute displaces for subblocks $j-1$ ($j = 2, 3, 4, 5$). Taking into account the width of the optical lines for the difference graphs in Fig. 20b (it gives an idea about the accuracy of the deformation measurements ≈ 2 μm), we can conclude that the main information of interest to us is contained in the records in the time interval up to 40-50 msec.

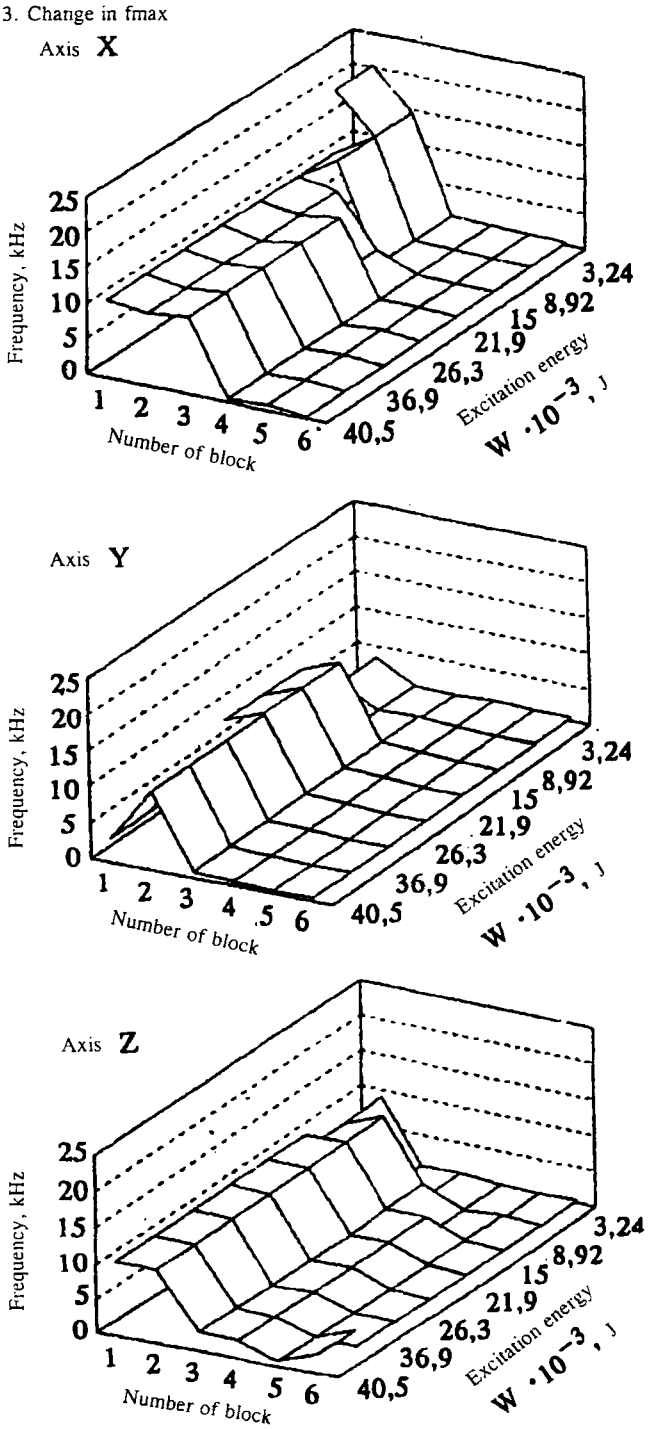

Fig. 23. Graphs of the dependence of parameter τ on pulse energy for directions (X, Y, Z) of blocks 1-6 of models 2, 3 in a three-dimensional representation.

In this connection, for a quantitative analysis it is convenient to use the graphs given in Figs. 21 and 22 with detailed records of respectively the absolute and relative displacements in time interval 0-40 msec. In these figures, left of the analog records (a) are given their spectrograms (b). As is easy to see from the graphs, the blocks inside the composite model have damped oscillatory movements as "absolutely" solid bodies in the manner of physical pendulums with amplitudes reaching 30 and more microns ($A_\mu \cong 3 \cdot 10^{-5}$ m). However, the spectrum of these oscillations is an order lower than for the low-frequency part of the spectral packets recorded by accelerometers (!). This fact is convincing confirmation of the assumption expressed

above that primarily dynamic intradeformation characteristics of the experimental blocks (say, soliton characteristics) are reflected on the records of the accelerograms. An analysis of the spectrograms for the graphs of the absolute and relative displacements of the blocks among themselves showed that spectral maxima (or modes) at frequencies 4.883, 7.766, 19.531, 39.066, 55, and 87 Hz are clearly detected on them. If we compose the ratios between adjacent values of the spectral maxima, then as a result we obtain:

$$\frac{78}{55} \cong 1{,}418 \cong \sqrt{2};\ \frac{55}{39{,}066} \cong 1{,}409 \cong \sqrt{2};\ \frac{39{,}066}{19{,}531} \cong 2{,}00 = 2;$$

$$\frac{19{,}531}{9{,}766} \cong 1{,}9999 \cong 2;\ \frac{9{,}766}{4{,}883} = 2.$$

That is, a rather rigorous fulfillment of canonical relation (6) is observed, but already for graphs of the absolute displacement of the blocks $A_\mu(t)$. Now let us compare the clearly expressed spectral packets for base frequency $f_0 \cong 10.65$ kHz, for the dominant "apparent" period $\hat{f}_0 \cong 0.49$ kHz (see Fig. 16: accelerograms of blocks 3-6; we will take the average of the spectral maximum 0.586 and 0.39 kHz), and for the dominant frequency $f_\mu \cong 20$ Hz for the carriers (blocks) of the pendulum wave. As a result of such a comparison we obtain a quite curious result. Namely: the ratios $f_0/\hat{f}_0$ and $\hat{f}_0/f_\mu$ are practically the same and equal to a value of the order of $(\sqrt{2})^9$. Inside the wave packets, as shown above, the spectral maxima are also related respectively with regard to f_0, $\hat{f}_0$, and f_μ according to formula (6). Evidently, the noted circumstance has a direct bearing on the effect of "self-reproduction" of the deformation picture in solid bodies at different scale levels, as follows from [5].

Since the indicated ratio of the frequencies f_0, $\hat{f}_0$, and f_μ has an obvious practical significance, we will give it a special notation

$$\chi = \mathrm{inv}(f_0/\hat{f}_0;\ \hat{f}_0/f_\mu) = (\sqrt{2})^9. \tag{8}$$

The following parameter important for practical applications is related to an evaluation of the amplitude values of the pendulum-type waves. Evidently, the geomechanical variant can serve as the "upper" bound [6]:

$$\mu_\Delta(\delta) = \delta/\Delta = \theta \cdot 10^{-2};\ \theta \in (0{,}5 \div 2). \tag{9}$$

The degree of maximum "freedom" of the geoblocks in the given case is estimated by the parameter δ, i.e., $A_\mu \leq \delta = \mu_\Delta(\delta)\cdot\Delta$. This characteristic is important for estimating the action of explosions in the near zone. For the "lower" bound of A_μ we will use the graphs of the relative displacements between blocks given in Figs. 20-22. Here the significant range of absolute displacement between blocks A_μ can be estimated by the interval 10-30 μm. The ratio of this interval to the longitudinal size of the blocks $\Delta = 0.125$ m is in the range

$$\frac{(10 - 30)\cdot 10^{-6}}{0{,}125} \in (0{,}8 - 2{,}4)\cdot 10^{-4} = \theta \cdot 10^{-4}. \tag{10}$$

In essence, depending on the stacking density of the blocks in the rock masses and energy of the pulsed action, the amplitude characteristics of the pendulum waves for the same carriers Δ "theoretically" can differ by two orders. Consequently, for the amplitude of pendulum-type waves A_μ with respect to displacements we can write the estimate

$$\mu_\Delta(\delta)\cdot\Delta\cdot 10^{-2} \leq A_\mu \leq \mu_\Delta(\delta)\cdot\Delta. \tag{11}$$

It is clear that under real conditions $A_\mu(t)$ depends on a number of geomechanical parameters, including on the distance and stress state of the masses and level of the energy action of the pulse sources.

An analysis of the graphs with respect to the characteristics of evolution of the spectra from subblock to subblock for the investigated models 2 and 3 (see Figs. 11-18) shows that the concepts "near," "middle," and "far" zones for pendulum waves with carriers Δ from pulse sources can be introduced completely concretely according to size. Thus, as the near zone from the pulse source we can take the region bounded by two Δ (high-frequency components of the spectrum dominate on the first two blocks); as the middle (or transition) zone we can take the region bounded by the distances from two to three Δ (the high- and low-frequency harmonics are comparable in amplitude in the third block); as the far zone we can take the region farther than 3Δ from the source (the high-frequency harmonics disappear). The noted features, as is seen from the oscillograms

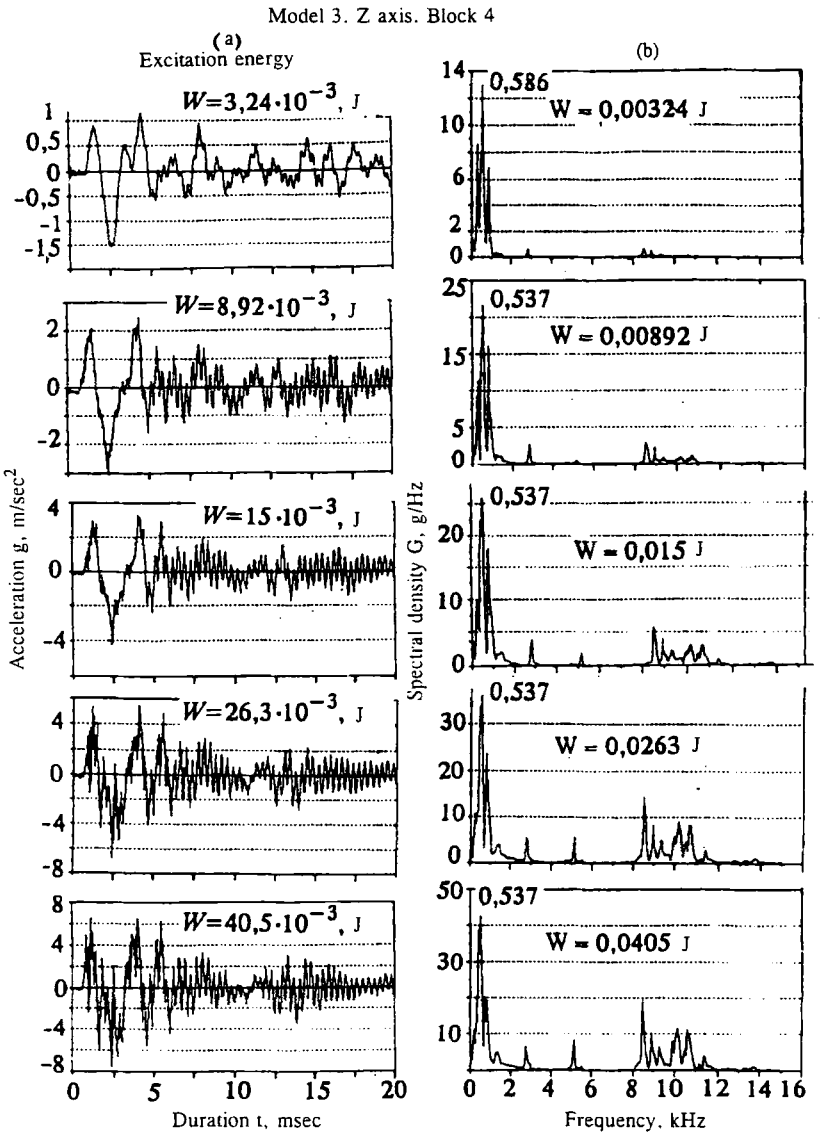

Fig. 24. Character of the evolution of the wave packet and its spectrum as a function of the pulse energy for the example of records for block 4 of model 3.

of the accelerometers given above are clearly traced not only in all three directions of recording the oscillations of the blocks of models 2 and 3 but also for blocks differing in composition (concrete, silicate brick, organic glass): it is necessary to call attention also to Figs. 2-3. In addition to differences in the spectral filling of these "zones," a distinct difference occurs also in the character of decay of the amplitude characteristic of the wave packets: within the first two zones it has an exponential dependence; on passing to the far zone decay practically ceases. Moreover, the amplitude of the pendulum waves can increase (!), evidently due to involvement into work of the weight of the overlying systems of blocks (Figs. 20-22).

As it seems to us, the known effect of the vibration action on oil and gas reservoirs in the light of the results noted above is due, evidently, to the propagation of precisely pendulum waves from the vibrators being used and not longitudinal and transverse waves. The latter are not only small in amplitude but also do not have the most important property of μ-waves toward weaker decay in the far zone (or even toward an increase of the amplitude of oscillations with distance).

We will now give an estimate of the propagation velocity of μ-waves for the example of model 3. This is easy to do on the basis of the records in Fig. 2 with respect to the delay $\Delta t \cong 1.67 \cdot 10^{-3}$ sec (block 5) of arrival of this wave and with respect to the distance between the surfaces of the first and fifth blocks $\Delta l = 4 \cdot 0.125 = 0.5$ m:

$$V_\mu = \frac{\Delta l}{\Delta t} \cong 300 \text{ m/sec} \tag{12}$$

Compared with the propagation velocity of longitudinal waves $V_p \cong 2662$ m/sec, this value of V_μ is quite small and comparable only with the speed of sound in air. The latter circumstance is of practical interest from the standpoint of estimating the effect, say, of underground explosions on the conditions of oscillations of air in mine workings: oscillations of the walls of workings can lead to a "piston" effect at the time of arrival of μ-waves. The comparability of the propagation velocity of air shock waves with velocity V_μ requires a special approach to an analysis of the appropriate experimental data from the standpoint of what is primary and what is secondary during the formation of air shock waves in underground workings. Only a combined spectral analysis of the results of measuring the pressure in air and oscillations in the rock mass can make a decisive contribution to understanding the essence here.

4. Let us turn now to the graphs of the dependence of parameter τ according to formula (1) on the energy of the pulsed action. Figure 23 shows the dependences in a three-dimensional representation for models 2 and 3 examined above (see also Figs. 4, 14, 18). The data given indicate that at certain levels of the energy actions the reverse process of a shift of the spectral densities into the high-frequency region occurs (in Fig. 4 this level is noted by a local minimum of parameter τ), i.e., secondary enrichment of the low-frequency wave packets with high-frequency harmonics with a simultaneous increase of their amplitude values occurs (strong slowing or stop of the increase of the amplitudes of low-frequency harmonics occurs). In essence, it is a question of the redistribution of the increasing energy from the external pulses in favor of high-frequency components (see Fig. 24, where the noted characteristics are illustrated for the example of records for the perpendicular direction of block 4 of model 3: on the left (a) are accelerograms and on the right (b) are spectral images). The canonical, according to type (6), character of the relation between harmonics which is preserved with increase of energy of the pulsed actions permits the assumption that at a certain critical value of the latter solitons in solid blocks due to reaching the limit tensile strains between them will be transformed into "true" subblocks (possibly, with disturbance of molecular bonds).

Since the dimensions of solitons are determined by the spectral energy distribution of elastic wave packets and propagation velocity of longitudinal waves V_p, it is natural to expect that at a critical energy of the external pulse breaking of the oscillating blocks into fractions whose size also obeys canonical relationship (6) can occur:

$$\vec{\Delta}_{\vec{i}} = \vec{\Delta}_0(\sqrt{2})^{\vec{i}};\ \vec{i} = (i_1, i_2, i_3);\ i_j = 0, -1, -2, -3, \ldots;$$
$$\vec{\Delta}_0 = (\Delta_1, \Delta_2, \Delta_3);\ (i_1, i_2, i_3) \leftrightarrow (x, y, z). \tag{13}$$

That is, under the effect of pulsed loads of sufficient energy in geomaterials and solid bodies (up to the critical point), crushing of the latter into fractions (subblocks) with sizes $\vec{\Delta}_{\vec{i}}$ obeying relationship (13) can occur. This agrees well with the data in [4] and generalizes the latter.

It is clear that sizes $\vec{\Delta}_{\vec{i}}$ will depend on the set of frequencies $\vec{f}_{\vec{i}} = (f_{i_1}, f_{i_2}, f_{i_3})$ on which "conversion" of solitons into real blocks in solid bodies is observed. The probability of such conversions evidently increases both with a decrease of distance to the place of applying the pulsed action and with an increase of the energy level of the latter.

In conclusion we will return to the curious effect noted by us above for the example of the records of accelerograms for block 3 of model 3 (Fig. 15) and indicating very weak damping of oscillations of the block perpendicular to the action of the pulse. In this case oscillations of the blocks in this direction after 5 msec become practically monochromatic (sinusoidal) at frequency 2.78 kHz (it is detected as a sharp spectral maximum in Fig. 15). In this sense the work of the mechanical system is an analog of the work of a laser system. The noted characteristic, as is seen in Fig. 24), occurs with a certain correction also on adjacent block 4 for the perpendicular direction.

If we assume that the effect of "disappearance" of friction between block 3 and adjacent blocks 2 and 4 is due to an "apparent" separation between the surfaces of these blocks (the latter can be imagined within the frameworks of notions about standing solitons) then on the basis of the formulas given above we can estimate the value of this "separation."

Actually, for solitons with frequency 2.78 kHz, which can be regarded as certain oscillating "blocks" inside the main block — the carrier of the pendulum wave (here we use the condition that we are dealing with standing solitons), by formula

$$\Delta \cong \frac{V_p}{(\sqrt{2})^9 \cdot 2f_0} \tag{14}$$

we can determine the linear size of the soliton $\Delta \cong 0.021$ m. Formula (14) is easily obtained from formula (8) and the analytical expression for the base frequency $f_0 = V_p/2\Delta$. In the given case $f_0 \cong 2780$ Hz (here it is taken into account that we are using the records of the accelerograms!). In accordance with the size of the solitons $\Delta \cong 0.021$ m, in conformity with estimate (10), their amplitude oscillations in standing waves are represented by the following range of values

$$(0{,}8 \div 2{,}4) \cdot 10^{-4} \cdot 2{,}1 \cdot 10^{-2} \text{ м} \in 2 \div 5 \ \mu\text{m}. \quad (15)$$

As we showed earlier in section 3 on the basis of optical measurements of the absolute and relative displacements of the blocks in the longitudinal direction, the given estimates (15) completely fit into the range of displacements obtained there experimentally, although (this is completely natural) slightly lower than their average values. In this connection, as it seems to the authors, the mechanisms of occurrence of rockbursts at coal, potassium, etc., deposits as well as rock bumps and earthquakes can be related most really to reaching critical conditions for the occurrence of the effect of anomalously low friction between beds of rocks or geoblocks. Hence also necessarily follows that a comprehensive study of the conditions of occurrence of the effect of anomalously low friction between interacting bodies should be regarded as the most important task of geomechanical investigations, since, obviously, major prospects in the area of technical applications (high-speed drilling and methods of driving works in strong rock masses without blasting, super-high-speed movements of solid bodies in liquid, solid, and gas media, creation of quiet assemblies and units, superplasticity of solid bodies, etc.) are related to the use of this phenomenon.

CONCLUSIONS

1. Investigations of physical modeling of pulsed actions on models of block media (with different material composition and characteristic dimensions of the subblocks) by energy-calibrated impacts confirmed the hypothesis expressed earlier by the authors about the possibility of existence of pendulum-type waves, the elementary carriers of which are geoblocks of a different scale level (μ-waves).

2. An analysis of the regularities of formation of the spectra of the wave packets and graphs of the absolute displacements of the blocks, determined by the optical method, permitted concluding a resonance mechanism of occurrence of μ-waves, underlying which is the canonical relationship of the spectral modes for wave packets with respect to factor $(\sqrt{2})^i$, $i = 0, \pm1, \pm2, \pm3, \ldots\ldots$

3. The effect of the condition of canonical relationship of the spectrum in wave packets of μ-waves under certain conditions of energy actions can leads to the occurrence of the effect of anomalously low friction between interacting blocks (carriers of μ-waves) in directions orthogonal to the line of action of the external pulse.

The work was performed with the financial support of the Russian basic research fund (grant No. 96-05-66052).

REFERENCES

1. M. V. Kurlenya, V. N. Oparin, and V. I. Vostrikov, "Pendulum-type waves. I: State of the problem and measuring and calculating complex," Fiz-Tekh. Probl. Razrab. Polezn. Iskop., No. 6 (1996).
2. V. N. Oparin, "Fundamentals of downhole geophysical flaw detection. I: Spectral analysis and measures of defectiveness," Fiz-Tekh. Probl. Razrab. Polezn. Iskop., No. 6 (1982).
3. L. D. Landau and E. M. Lifshits, Theoretical Physics. Vol. 7: Elasticity Theory [in Russian], Nauka, Moscow (1987).
4. V. N. Oparin and M. V. Kurlenya, "Gutenberg velocity section of the earth and its possible geomechanical explanation. I: Zonal geodisintegration and hierarchical series of geoblocks," Fiz.-Tekh Probl. Razrab. Polezn. Iskop., No. 2 (1994).
5. M. V. Kurlenya and V. N. Oparin, "Scale factor of the phenomenon of zonal disintegration of rocks and canonical series of atomic and ionic radii," Ibid., No. 2 (1996).
6. M. V. Kurlenya, V. N. Oparin, and A. A. Eremenko, "Ratio of linear dimensions of rock blocks to the width of opening of fractures in a structural hierarchy of rock masses," Ibid., No. 3 (1993).